Identifying Vulnerabilities and Novel Drug Candidates in Platinum-Resistant Ovarian Cancer.

Identifying Vulnerabilities and Novel Drug Candidates in Platinum-Resistant Ovarian Cancer.

Chiara Victor

A Thesis in the Field of Bioengineering and Nano Technology

for the Degree of Master of Liberal Arts in Extension Studies

Harvard University

May 2024

Abstract

Ovarian cancer is the fifth leading cause of female, cancer-related death in the United States and the deadliest form of gynecological cancer (Cancer Facts & Figures 2022, 2022). Epithelial ovarian cancer (EOC) accounts for 90% of all diagnosed ovarian cancers, 70% of which are High Grade Serous Ovarian Cancer (HGSOC), with a five-year survival rate less than 25% (Cai et al., 2014; Ediriweera et al., 2019; Iyengar et al., 2018; Lisio et al., 2019; Siwak et al., 2010). Platinum-taxane combination therapy has been the standard of care since its introduction in the 1990s yet, over 70% of HGSOC patients relapse due to platinum resistance (PR) (Kim et al., 2012; Kristedja et al., 2010; Moghbeli, 2021). There is a critical need for alternative therapeutic options for PR HGSOC. Here, we aimed to generate models of PR from HGSOC cell lines intrinsically sensitive to cisplatin and screen them against a panel of 225 small molecule inhibitors. The panel consists of FDA-approved drugs currently being used clinically, drugs in Phase II or III clinical trials, as well as novel-preclinical small molecule kinase inhibitors and tool compounds to identify single agents and/or pathways of interest in combating PR. Aligning with previous research, selective EGFR and PI3K inhibitors elicited significant responses in the PR model compared to the parental cell line. Lastly, the MEK inhibitor, cobimetinib, displayed advantageous responses in the PR model and highlight the MEK pathway to be further investigated in the context of PR HGSOC.

Acknowledgments

The work presented here would not have been possible without the support of Dr. Peter Sorger and the of the Laboratory of Systems Pharmacology at Harvard Medical School. Many thanks to Dr. Peter Sorger and his mentorship throughout the entirety of this process. To Dr. Caitlin E. Mills, thank you for the continuous guidance and advice you provided at every step throughout the experimental and writing portions of this thesis as well as all of the time invested into seeing this project to it's completion.

Table of Contents

List of Tables

List of Figures

Chapter I.

Introduction

Ovarian Cancer Background and Current Treatment Strategies

Ovarian cancer is the fifth leading cause of female, cancer-related death in the United States and the deadliest form of gynecological cancer (Cancer Facts & Figures 2022, 2022). Ovarian cancer encompasses a wide range of tumor types classified by origin with Epithelial Ovarian Cancer (EOC) accounting for 90% of all diagnosed cases. EOC is further classified into serous, endometrioid, mucinous, and clear cell subtypes (Ediriweera et al., 2019; Iyengar et al., 2018; Siwak et al., 2010). Seventy percent of diagnosed cases are High Grade Serous Ovarian Cancer (HGSOC), a histological subtype of EOC, that has a five-year survival rate less than 25% (Cai et al., 2014; Iyengar et al., 2018; Lisio et al., 2019). The high incidence and poor-prognosis of HGSOC can be attributed to lack of symptoms and lack of effective screening methods which lead to late-stage detection and limited therapeutic options (Michels et al., 2013).

The initial treatment strategy for HGSOC is surgical "debulking" with the goal of completely resecting all tumor matter. The probability of complete resection, especially in metastasized HGSOC, is low but if the surgery is successful, overall survival (OS) rates increase (Lisio et al., 2019). However, regardless of tumor debulking success, essentially all HGSOC patients undergo chemotherapy (Lisio et al., 2019). Since its introduction in the 1990s, a chemotherapeutic platinum-taxane combination therapy using cisplatin or carboplatin with paclitaxel has been the standard of care for all ovarian cancer diagnoses (Banerjee & Kaye, 2013; Peng et al., 2010).

Cisplatin binds to the purine residues of DNA causing single and double-strand breaks resulting in S/G2 cell cycle arrest and apoptosis, while paclitaxel induces apoptosis through arrest in the G2/M-phase of the cell cycle by inhibiting microtubule depolymerization (Dasari & Tchounwou, 2014; Kampan et al., 2015). Despite eliciting initial cytotoxic responses, over 70% of patients with HGSOC experience disease relapse and platinum resistance (PR) with a median progression-free survival (PFS) rate of 18 months and 5-year survival rate around 25% (Kim et al., 2012; Kristedja et al., 2010; Moghbeli, 2021).

There are two approved alternative treatment options for PR HGSOC but the effects on PFS and 5-year survival are modest. First, the poly (ADP-ribosyl) polymerase (PARP) inhibitor Olaparib is approved by the Food and Drug Administration (FDA) for the treatment of BRCA mutated PR HGSOC and although eliciting high objective response rates (ORR) compared to the standard of care, recent data collected in the clinic suggests no significant difference in PFS (Vanderstichele et al., 2019). The second FDA approved treatment is Bevacizumab, a monoclonal anti-vascular endothelial growth factor (VEGF) inhibitor, used in combination with chemotherapy, which was approved in 2014. In a phase III clinical trial, the Bevacizumab/chemotherapy combination increased PFS two-fold in comparison to chemotherapy alone (about 3.5 months increase) although no significant improvement in OS was found and serious side effects are a concern for this therapeutic option in the clinic (McClung & Wenham, 2016).

Given (i) the initial strong responses to platinum-based therapies, (ii) how common the acquisition of platinum resistance is, and (iii) the limited number (and poor performance) of alternative treatments, there is a critical need for further research into

mechanisms of resistance and strategies to extend the benefits of platinum-based therapies.

Mechanisms of Resistance to Platinum-Based Drugs

Despite platinum therapies being widely used in cancer treatment, and resistance being a common obstacle in their use, how platinum resistance arises is not fully understood, and strategies to overcome it are still needed (Galluzzi et al., 2012; Sima et al., 2018; S. Wang et al., 2015; Xu et al., 2021; Yang et al., 2020). There are numerous mutations and alterations in cell cycle regulation and proliferation that investigators have suggested as possible causes of resistance (outlined below) that can be categorized as genetic and non-genetic modes of resistance (Christie et al., 2017; Shaffer et al., 2017).

Genetic mutations have been found to contribute to intrinsic and acquired resistance in HGSOC. The tumor suppressor, p53, is activated by DNA damage and promotes cell cycle arrest and apoptosis. p53 mutations are common in HGSOC and are a known mechanism of intrinsic resistance by altering the downstream signaling pathways activated by platinum-induced DNA damage (Fraser et al., 2008).

Mutations in BRCA1/2 can lead to homologous recombination repair (HR) deficiency which is common in HGSOC. While HR-deficient tumors exhibit strong initial responses to platinum, acquired resistance to platinum compounds can result from secondary mutations in BRCA1/2 that reestablish HR repair proficiency (Galluzzi et al., 2012; Song et al., 2022; J. Wang et al., 2017; J. Zhang et al., 2013). The reestablishment of HR-proficiency can also lead to resistance to drugs targeting the other repair mechanisms such as PARP inhibitors.

Changes in gene expression can result from genetic mutations and non-genetic alterations. Overexpression of EGFR or MKP-1 have been linked to intrinsic resistance to cisplatin (J. Wang et al., 2017; Wee & Wang, 2017). Overexpression of EGFR family members results in increased activation of the RAS/MEK/ERK and PI3K/Akt/mTOR pathways, which leads to increased cell proliferation (Poursheikhani et al., 2020; Wee & Wang, 2017). EGFR overexpression and PR are highly correlated in HGSOC, and the consensus in the field is that overexpression of the EGFR family is correlated with poor prognosis (Cai et al., 2014; Dasari & Tchounwou, 2014; Fraser et al., 2008; Iyengar et al., 2018; Kampan et al., 2015; Kim et al., 2012; Moghbeli, 2021; Song et al., 2022; Yang et al., 2020). MKP-1 (DUSP1), a key phosphatase in the mitogen-activated protein kinases (MAPK) family has been associated with PR, with increased MKP-1 levels found in PR HGSOC compared to their platinum-sensitive counterpart in vitro (Fraser et al., 2008; Song et al., 2022).

Cellular mechanisms that decrease the accumulation of platinum compounds in the cell thereby resulting in the drug not reaching its target, can also contribute to acquired PR. Generally, this is achieved by increased drug efflux and thereby detoxification carried out by ABC membrane transporters, commonly referred to as the multi-drug resistance phenomena (Song et al., 2022). On the contrary, it has also been reported that this is not a factor in PR and rather decreased intracellular accumulation is the result of decreased uptake rather than increased outflow (Galluzzi et al., 2012). Additionally, increased nucleophilic substances which bind to platinum compounds such as glutathione, essentially quenching its effect, have been correlated with PR (Song et al., 2022).

Furthermore, changes in how cells respond to DNA damage inflicted by platinum compounds can also contribute to acquired resistance. Defects in nucleotide excision repair (NER), Mismatch Repair and Homologous recombination (HR) repair processes can all lead to PR. In NER, ERCC1 can repair adducts in the DNA formed by platinum compounds and increased ERCC1 levels have been correlated with resistence (Song et al., 2022). Here, the drug reaches its target; however, the cells are able to reverse its effects.

Treatment Strategies in PR HGSOC

Given the prevalence of PR in ovarian cancer patients, numerous strategies and pathways have been investigated to circumvent PR. Here, EGFR/HER inhibition and inhibitors, PARP inhibitors, and PI3K/mTOR/Akt pathway inhibitors are highlighted and their treatment potential in the context of HGSOC is discussed.

EGFR/HER inhibition

The prevalence of EGFR overexpression in HGSOC and its association with PR has led researchers targeting this family of receptors. The family includes EGFR (ERBB1), HER2 (ERBB2), HER3 (ERBB3) and HER4 (ERBB4). HER2 overexpression occurs in approximately 30% of all ovarian cancers, while EGFR overexpression reports vary, ranging from 13% to 98% (Galluzzi et al., 2012; Momeny et al., 2017; Siwak et al., 2010). EGFR inhibitors have been evaluated as single agents and in combination with chemotherapy in clinical trials in ovarian cancer with minimal to no clinical gain (Siwak et al., 2010; Wilken et al., 2012). However, EGFR overexpression was not a criterion for inclusion in these trials nor was platinum resistance.

EGFR/HER Inhibitors

Despite poor performance in trials, small molecule EGFR family inhibitors have shown preclinical promise in resensitizing PR HGSOC cell lines to platinum treatment. (Galluzzi et al., 2012; Sima et al., 2018; S. Wang et al., 2015; Xu et al., 2021; Yang et al., 2020). Dacomitinib and Afatinib are FDA-approved pan-ERBB inhibitors that irreversibly bind to EGFR, HER2, and HER4. Both of these drugs were found to increase cisplatin-induced apoptosis, suggesting a synergistic mechanism of action in ovarian cancer cell lines (S. Wang et al., 2015; Xu et al., 2021). Furthermore, in a comprehensive drug screen of 2606 approved small molecule drugs in a cisplatin-resistant A2780 ovarian cancer cell line model, the top five drug hits for cell killing were EGFR family inhibitors (Sima et al., 2018). Of these, CUDC-101, WZ4002, varlitinib, and canertinib, resensitized the resistant model to cisplatin (Sima et al., 2018). While on-target efficacy was confirmed by decreased p-EGFR expression for dacomitinib, afatinib, and CUDC-101 in combination with cisplatin, it does not preclude the possibility that targets other than EGFR were responsible for the resensitization to cisplatin (Sima et al., 2018; S. Wang et al., 2015; Xu et al., 2021; Yang et al., 2020).

Therefore, in order to draw a causal claim of the effect EGFR inhibition has on resensitizing PR cells to cisplatin, one group performed an experiment using small interfering RNAs to knockdown EGFR expression in a platinum resistant model of ovarian cancer. This resulted in partial recovery of cisplatin's efficacy, which supports their claim that on-target effects of small molecule EGFR inhibitors lead to the resensitization of the resistant model to cisplatin (Sima et al., 2018).

Interestingly, it was suggested that, in addition to on-target effects measured by decreased p-EGFR and p-HER2 expression, afatinib also mitigated multidrug resistance (phenomenon explained above) by decreasing the expression of ABCB1 (Galluzzi et al., 2012; S. Wang et al., 2015). However, cisplatin has not been shown to be a MDR1 substrate, and its upregulation has not been linked to cisplatin resistance (Ren et al., 2007; Sherman-Baust et al., 2011). Taken together, these results suggest afatinib as a potential therapeutic option in the clinic given that it can resensitize both EGFR-mutated and non-mutated PR HGSOC, either by its nominal or off-target effects.

Furthermore, taking a bioinformatics approach, Yang and colleagues (2020) performed differential expression analysis (H. Wang et al., 2015) to identify significantly differentially expressed genes between cisplatin sensitive and resistant cell lines from the National Center for Biotechnology Information's, Gene Expression Omnibus (GEO) database. Through this analysis, EGFR and ERBB2 overexpression were identified in the resistant cell lines and suggested to be druggable targets for PR (Yang et al., 2020).

PARP Inhibitors

Olaparib, rucaparib, and niraparib are FDA-approved PARP inhibitors used in the treatment of ovarian cancer. PARP inhibitors work by inhibiting base excision repair, which repairs single-strand breaks in the DNA, pushing them towards the HR repair system which is often deficient in HGSOC as a result of BRCA mutations (Cooke & Brenton, 2011; Konstantinopoulos et al., 2015; Michels et al., 2013; Song et al., 2022; J. Wang et al., 2017). Additionally, as previously mentioned, secondary mutations that reestablish HR function are common, with one study finding secondary mutations in 46% of PR ovarian cancers (Konstantinopoulos et al., 2015). Therefore, PARP inhibition is

only a viable strategy for patients who acquire PR via mechanisms other than HR-proficiency.

It has also been suggested that PARP inhibitors could be used to treat MKP-1 high PR ovarian cancers (J. Wang et al., 2017). Both MKP-1 and PARP have been reported to be elevated in the PR setting; MKP-1 overexpression has been reported to stimulate PARP-1 expression, and MKP-1 silencing via short hairpin RNA was found to result in increased PARP ubiquitination and degradation (J. Wang et al., 2017). Moreover, cisplatin was found to induce more cell death if MKP-1 was silenced (J. Wang et al., 2017). As a consequence, there is interest in directly targeting MKP-1 (DUSP1) as well as continued interest in identifying the best way to incorporate PARP inhibition in the treatment of HGSOC (Sanders et al., 2022). This finding suggests PARP inhibitors could work on multiple pathways of resistance in HGSOC and have the potential to be a therapeutic option in non-BRCA mutated HGSOC.

Administering PARP inhibitors in combination with cisplatin is yet another application that has been explored. Zhang and colleagues (J. Zhang et al., 2013) found the PARP inhibitor 3-AB, to be more efficacious in PR ovarian cancer when used in combination with cisplatin and characterized their mechanism of action as resensitizing the cells to cisplatin. Although, additional research is needed to investigate the combination of cisplatin and PARP inhibitors as well as the role PARP inhibitors play in combating PR.

PI3K/Akt/mTOR Pathway Inhibitors

The PI3K/Akt/mTOR pathway plays an important role in cell proliferation. When PI3K is activated by growth factors, it initiates the phosphorylation of PIP2 to PIP3,

which binds to and activates Akt. Once activated, Akt can directly or indirectly activate mTOR leading to protein synthesis and cell proliferation (Ediriweera et al., 2019; Peng et al., 2010). Although there is an abundance of preclinical evidence outlining the importance of this pathway in EOC, no targeted therapies have been approved despite approvals for other indications (Cai et al., 2014; Deng et al., 2019; Ediriweera et al., 2019; Fraser et al., 2008). For example, Akt inhibitors as a combination treatment for hormone sensitive prostate cancer, metastatic prostate cancer, triple negative breast cancer and numerous classes of metastatic breast cancer are in phase III clinical trials (Hua et al., 2021). In 2023, the FDA approved a combination treatment with an Akt inhibitor (capivasertib) for HR+/HER2- locally advanced or metastatic breast cancer (Mullard, 2024).

The PI3K/Akt/mTOR inhibitors, BEZ235, PI-103 and RY-2F were evaluated as single agents and BEZ235 and PI-103 in combination with cisplatin, in HGSOC cell lines. PI-103, elicited no significant effect when used as a single agent in the SVOV3-PR model but when used in combination with cisplatin, growth inhibition was increased dose-dependently (Cai et al., 2014). Similar results were found in the evaluation of BEZ235: in combination with cisplatin, it resulted in increased killing of PR ovarian cancer cell line models as compared to either therapeutic alone, as measured in the clonogenic assay and by direct measurement of apoptotic cells (Deng et al., 2019).

Methods of Analyzing Dose Response

Conventionally, IC_{50}, E_{max}, and AUC values have been produced using well-average viability assays to compare cell counts for drug-treated and control conditions but it has been shown that IC_{50}, E_{max}, and AUC values are heavily skewed by cell

proliferation and this variability increases in experiments with longer timepoints (Hafner et al., 2016; Mills et al., 2022). For example, the majority of previous data presented is based on preclinical results in SKOV3 and A7280 EOC cell lines (Cai et al., 2014; Deng et al., 2019; Momeny et al., 2017; Sima et al., 2018; J. Wang et al., 2017; S. Wang et al., 2015). Taking an average of published doubling rates of these cell lines, A2780 proliferates two times faster than SKOV3. This difference in baseline growth rates results in dramatic variations of IC_{50} and E_{max} values, leading to skewed data comparisons and inaccurate conclusions (Hafner et al., 2016; Mills et al., 2022). Growth rate bias can be mitigated by correcting for variable division rates across cell lines using Growth Rate inhibition (GR) metrics (Hafner et al., 2016). Since comparisons between cell lines with different growth rates are central to this thesis, GR_{50}, GR_{max} and GR_{AOC} were used in place of IC_{50}, E_{max} and AUC, respectively. GR metrics normalize results for cell proliferation thereby making drug responses across cell lines directly comparable and increasingly translational (Hafner et al., 2016, 2017; Mills et al., 2022; Niepel et al., 2019).

When performing large-scale screens, there is a trade-off between aspects including but not limited to throughput, cost, ease of use, and desired readouts. CellTiter-Glo® is a common assay used for high-throughput screens due to its low cost and minimal-step workflow; leveraging luminescence derived from ATP to evaluate cell viability (Noah et al., 2007). However, advances have been made in developing microscopy-based multiplexed assays for high-throughput experiments to enhance the readouts derived from these large-scale experiments and provide increasingly thorough insight for follow-up experiments, such as cell-painting for fixed cell assays and

EllipTrack for live cell assays (Bray et al., 2016; Tian et al., 2020). Another important confounder in high-throughput screens is reproducibility. Niepel and colleagues (2019) found that in addition to variability of cell line proliferation, irreproducibility of immunofluorescence assays was common, due in part to uneven cell loss caused by cell disruption during the multi-step staining protocol.

Recently, the Deep Dye Drop (DDD) protocol was published (Mills et al., 2022). This protocol is low cost, minimizes cell disruption during the staining protocol and is applicable to high-throughput screens. Additionally, the DDD staining protocol allows for single-cell data, providing more precise results compared to well-average viability assays like CellTiter Glo® (Hafner et al., 2016; Mills et al., 2022). Furthermore, this protocol is compatible with downstream GR analysis which normalizes for differences in cell proliferation rates between cell lines, a known confounder in comparative dose response studies (Hafner et al., 2016; Niepel et al., 2019).

Research Aims, Goals, and Hypothesis

This thesis includes two primary goals: (1) to establish HGSOC cell line models of acquired cisplatin resistance, and (2) to identify targeted inhibitors that are more effective in PR cell lines than in parental control lines. To accomplish these aims, comprehensive profiling of 34 HGSOC cell lines treated with a panel of 35 drugs was leveraged for three purposes: 1) to investigate intrinsic sensitivity to cisplatin by looking at the range of responses across different cell lines; 2) to identify potential vulnerabilities in PR cells by looking for drug responses that are negatively correlated with cisplatin response across our HGSOC cell line panel; and 3) to identify cisplatin-sensitive cell lines that can be used to generate acquired-resistance models. Following establishment of

the acquired PR models, a comprehensive screen of 225 small molecule kinase inhibitors will be performed in one or more paired platinum-resistant/parental cell lines to identify potential targets for PR-HGSOC. Lastly, data from both the HGSOC cell line panel and the screen in the PR model(s) will be leveraged to explore if drugs identified as being negatively correlated with cisplatin are efficacious in a PR model. I hypothesize that the acquisition of cisplatin-resistance will sensitize the cells to other targeted therapies. More specifically, based on previous literature, it is hypothesized that inhibitors targeting the EGFR, PARP, and PI3K/Akt/mTOR pathway will have the greatest differential in models of acquired PR. To assess the hypothesis, three aims will be used to address the primary goals. Details of the Study design can be found in the methods section.

Primary goals: Identify cisplatin-sensitive cell lines that can be used to generate acquired-resistance, investigate intrinsic sensitivity to cisplatin and identify vulnerabilities in PR.

Specific Aim 1: Investigate the heterogeneity in responses of HGSOC cell lines to small molecule targeted therapies.

Methods: Analyze an existing dataset in which 34 OC cell lines were treated with a panel of 34 drugs at nine concentrations. The drug panel included clinically relevant CDK inhibitors, PI3K/AKT/mTOR inhibitors, PARP inhibitors as well as common chemotherapeutic agents including cisplatin.

Expected Results: Quantify cell line sensitivity to cisplatin and potential vulnerabilities *in vitro*. There will be a wide range of responses to cisplatin across the panel of HGSOC; the most sensitive lines will be used in specific aim 2. There will be a wide range of correlations between responses to cisplatin and responses to other drugs in the panel; drugs

negatively correlated with cisplatin sensitivity will be tested in the PR lines in specific aim 3.

Specific Aim 2: Generate PR cell line models from cisplatin-sensitive cell lines to be used in the drug screen.

Methods: chronically expose cisplatin-sensitive cell lines to increasing concentrations of cisplatin in the media.

Expected results: over time, cell lines will grow resistant to cisplatin and sustain proliferation in the presence of doses up to 3 μM cisplatin.

Specific Aim 3: Identify vulnerabilities in PR-OVCA in vitro.

Methods: Screen the PR cell lines established in specific aim 2 and their parental controls with the panel of drugs used in the ovarian cancer profiling project (OvCa-L) as well as the Optimal Kinase Library (OKL) (Moret et al., 2019).

Expected results: PR generated cell lines show a range of effects in response to target kinase inhibitors from cross resistance to hypersensitivity. PR lines are expected to be sensitive to drugs negatively correlated with cisplatin in the OvCa profiling project as well as inhibitors targeting the EGFR, PARP, and PI3K/Akt/mTOR pathways.

Chapter II.

Materials and Methods

Resistant Cell Line Generation

Four parental HGSOC cell lines (Table 1) were selected to generate cisplatin resistant models based on three criteria: 1) the cell lines were sensitive to cisplatin with GRAOC > 0.55; 2) the four cell lines were all different subtypes which helps to account for the heterogeneity within the HGSOC subtype; 3) the selected cell lines were considered accurate cell line models of HGSOC seen in the clinic based on their molecular profiles34. Each cell line's cancer origin, GRAOC of cisplatin, growth media and seeding density in 384 well plates is shown in Table 1.

Table 1. Cell Line selection for PR Models

Cell Line	Cancer Type	GRAOC of Cisplatin	Seeding Density/well	Growth Medium and Additives
RMUGS	Ovarian mucinous cystadenocarcinoma	0.6	750	Ham's F12 +10% FBS, 1% P/S
SNU8	Ovarian serous cystadenocarcinoma	0.8	750	RPMI 1640 + 25mM HEPES, 10% FBS, 1% P/S
59M	High grade ovarian serous adenocarcinoma	0.7	1000	DMEM + .02IU/ml BI, 10%FBS, 1% P/S
JHOS4	High grade ovarian serous adenocarcinoma	1	1000	DMEM/HamF12 (1:1) + 0.1mM NEAA, 10% FBS, 1% P/S

Table 1 includes Cell line indication, GRAOC Response to Cisplatin from the OvCa Profiling Project, Growth Media Conditions and Seeding Density for a 96-well plate. Abbreviations; Dulbecco's Modified Eagle Serum (DMEM), Fetal Bovine Serum (FBS), Penicillin-Streptomycin (P/S), Bovine Insulin (BI), Roswell Park Memorial Institute 1640 (RMPI), Non-Essential Amino Acids (NEAA).

All cell lines were cultured in their recommended media conditions (Table 1) at 37°C and 5% CO2, and were identity verified via Short Tandem Repeat profiling (Masters et al., 2001). To create the resistant models, cell lines were chronically exposed to cisplatin over six months by adding cisplatin into the culture media, starting at a concentration of 0.5 μM and increasing every 2-3 weeks, as the cells allowed, in the hopes of reaching adequate cell proliferation in the presence of 3 μM cisplatin-containing media.

Resistance was assessed by treating the parental lines and their resistant counterparts with cisplatin in a 9-point dose response format in technical and biological triplicates. Cells were seeded in 384-well Perkin Elmer CellCarrier® plates and left to adhere for 24 hours prior to drug treatment via D300 digital drug dispenser. After the addition of the drugs, the treatment plates were placed back in incubators at 37°C and 5% CO_2 for 144 hours (6 days). At the same time as drug treatment, time=0 plates were stained and fixed according to the DDD protocol (see below). Time=0 plates were used as a benchmark for evaluating cell proliferation and used to calculate normalized GR values. After 144 hours, the treatment plates were stained following the same process and all plates were imaged.

Jupyter notebooks were used to access custom experimental design and data analysis tools to generate randomized, dose response treatment (and metadata) files for dispensing cisplatin with the D300 digital drug dispenser.

Drug Library Screen and Validation Experiments

The initial screen (see below for a description of the libraries) of PR versus parental cells was conducted in biological and technical triplicate. Cells were plated in

384-well plates as described above, and were subjected to the same DDD staining protocol and image acquisition as the previously described dose-response experiments in 'Resistant Cell Line Generation' with one exception; the plates were treated with drugs via pin transfer using an Epson robot at the ICCB-L screening facility at Harvard Medical School rather than the D300 digital drug dispenser.

Validation experiments were performed in biological duplicate and technical triplicate using the D300 to dispense drugs at nine concentrations covering four orders of magnitude in half-log dilution series from 10 μM to 10 nM that hit in the screening stage of the project.

Small Molecule Inhibitor Libraries

The two drug panels used in the screening experiments included the library used in the ovarian cancer profiling project (OvCa-L) consisting of 33 drugs as well as the Optimal Kinase Library (OKL) provided by the ICCB Longwood Medical Facility, which consists of 192 kinase inhibitors (see Appendix, Table 5). The drugs included in the panel are FDA-approved drugs currently being used clinically, drugs in Phase II or III clinical trials, as well as novel-preclinical small molecule kinase inhibitors and tool compounds covering the pathways outlined previously such as EGFR, PARP, and PI3K as well as the rest of the kinome (Moret et al., 2019). The OvCa-L included each drug at nine concentrations covering four orders of magnitude in half-log dilution series from 10 μM to 10 nM while the OKL included 4 doses in 1:10 dilution series from 10 μM to 10 nM.

Analysis of KINOMEscan Data

KINOMEscan affinity data (Davis et al., 2011) for 395 wildtype kinases and 73 mutant kinases were available for all compounds in the Optimal Kinase Library at four concentrations (Moret et al., 2020). KINOMEscan data are a percent control measurement for each inhibitor-target pair: a percent control value of 100 indicates no binding whereas a value of 0 indicates strong inhibition of that target. The 100 nM KINOMEscan data for each screening hit was filtered to keep only the wildtype kinases, and then further filtered to only include those kinases with a % control value below 10% for at least one hit. The resulting dataset was then clustered by kinase and inhibitor using the Seaborn clustermap function in Python.

Deep Dye Drop Protocol

To perform the Deep Dye Drop (DDD) assay, Hoechst was used to stain all nuclei, LIVE/DEAD Red (L/DR) to stain dead cells, and EdU labeled with Sulfo-cy3 azide (Cy3) to stain cells in S phase as described previously (Mills et al., 2022). Fifteen microliters of a 1X Phosphate Buffered Saline (PBS) solution containing 10% Optiprep, EdU (1:1000) and L/DR (1:2000) was added to each well and left to incubate 37°C. After one hour, the cells were removed from the incubator and 20 µl of a PBS solution containing a final concentration of 20% Optiprep and 4% formaldehyde were added to each well and left to incubate in the dark at Room Temperature (RT). After 30 minutes, the wells were aspirated, washed with 80 µl/well of PBS and subsequently aspirated using a EL406 plate washer.

Next, the cells were permeabilized by adding 15 µl of a PBS solution containing 10% Optiprep and 0.5% Triton X-100, left to incubate in the dark at RT. After 20

minutes, a click reaction was used to label EdU with Cy3 by adding 20 µl of a PBS solution containing 20% Optiprep to each well with the following reagents added to the Optiprep/PBS solution in order; 2 mM final concentration of Copper(II) sulfate (CuSO4), 4 µM final concentration of Cy3, and a 20 mg/mL final concentration of ascorbic acid. After incubation at RT in the dark for 30 minutes, each well was aspirated, washed with 80uL PBS and aspirated again using the plate washer.

Following this, 40 µl/well of Odyssey blocking buffer was added and left to incubate at RT, in the dark, on a low-speed orbital shaker. After one hour, each well was aspirated using the plate washer and 15 µl of Odyssey blocking buffer containing Hoechst 33342 (1:5000) was added to each well. The plates were then sealed with foil seals and left to incubate overnight at 4°C on a low-speed orbital shaker. The next day, the plates were washed with PBS containing 0.01% tween, twice with PBS (with aspirations in between each wash) followed by 80 µl of PBS dispensed and left in each well. Once this last washing step was complete, the plates were sealed with foil seals and stored at 4°C until imaging.

Immunofluorescence Imaging

Plates were imaged using an ImageXpress® Micro-Confocal (IXM-C) high throughput microscope with a 10x objective; four fields of view were imaged per well nearly covering the full well area. Nuclei were segmented based on their Hoechst signal using MetaXpress® software, and a four-pixel ring was drawn around each nucleus. Intensity values for Hoechst, L/DR and EdU within the nuclear area (minus the local background intensity from the four-pixel ring) were saved at the single cell level DNA content. Based on intensity readouts of Hoechst, live cell counts as well as cells in either

the G1 or G2-phases of the cell cycle were acquired. EdU allowed recognition of cells in S-phase and L/DR for dead cell counts.

Growth Rate Inhibition Metrics

Using the intensity outputs of Hoechst, L/DR and EdU from MetaXpress combined with a metadata file, we obtained GR metrics. Once all GR metrics are calculated using Jupyter notebook scripts, the following analyses were carried out in Microsoft Excel. All GR related resources are open source and available online.

Cell line Generation and Validation Experiments

For the purpose of this experiment, the ratio of growth rate inhibition between the treatment and control conditions was used to evaluate the inhibitory effects of cisplatin on the parental (control) and resistant (treatment) models in order to quantify resistance. The mean growth rate inhibition (GR value) of technical triplicates for each concentration (mean GR value) was used to calculate the difference in GR values (GR_{C-P}) between the cisplatin-resistant (GR_C) and parental (GR_P) cells for each cell line, at each concentration.

$$GR_C - GR_P = GR_{C-P}$$

Because a lower GR value represents a stronger inhibitory effect, GR_{C-P} was calculated in this manner to generate positive GR_{C-P} values that are more intuitive.

Library Screen

To identify drug hits for further evaluation in validation experiments, screening results were analyzed using two sequential methods. First, the area over the GR curve

(GR_{AOC}) metric was used to identify drugs that had stronger effects in the resistant model compared to its parental counterpart. A larger GR_{AOC} value represents a stronger response to the given drug. Therefore, we calculated the difference in GRAOC by subtracting GR_{AOC} of the parental line ($GRAOC_P$) from GR_{AOC} of the resistant line ($GRAOC_C$).

$$GRAOC_C - GRAOC_P = GRAOC_{diff}$$

Drugs with a $GRAOC_{diff} \geq 0.20$ consistent across biological replicates were considered preliminary hits and included in further analysis.

Next, the mean GR values were used to further evaluate growth rate inhibition for each preliminary hit. The purpose of this analysis step was to rank the long list of drug hits based on their inhibitory effect with respect to concentration. Because a lower GR value represents a stronger inhibitory effect, the difference in GR values (GR_{P-C}) between the parental (GR_P) and resistant (GR_C) model for each cell line, at each concentration was calculated by subtracting GR_C from GR_P.

$$GR_P - GR_C = GR_{P-C}$$

Calculating GR_{P-C} for this analysis resulted in positive values when the cisplatin-resistant line responded more strongly than the parental control line.

Statistical Analysis

All GR values for cell line quality control (QC), screening and validation results were analyzed by taking the mean and standard error of the technical replicates of each biological replicate. QC of PR cell lines were analyzed using a paired t-test between the PR and parental lines. A p-value ≤ 0.05 was considered significant and denoted that cell line to be used in the screening and validation experiments. GR_{AOC} and GR_{50}, exported from Jupyter Notebook scripts, were used to evaluate the OvCa Profiling data. To

identify the potential vulnerabilities of PR to drugs in the OvCa profiling project, a spearman r correlation was used to assess the negative correlation between cisplatin and the drugs in the OvCa-L a spearman $r \leq -0.3$ considered a significant negative correlation to cisplatin. paired t-tests were performed for the validation experiments to compare the parental and resistant lines' GR_{max} and GR_{AOC} of each drug.

Chapter III.

Results

OvCa Profiling

Sensitivity to cisplatin was previously found to be variable in potency (GR_{50} values from 0.02 μM to 6.27 μM) and efficacy (GR_{max} values from -0.75 to 0.01) across a panel of 30 HGSOC cell lines and four non-malignant controls (Figure 1a). The area over the GR curve (GR_{AOC}), a good measure of overall sensitivity, was found to vary from 0.07 to 0.84. The 59M, RMUGS, JHOS-4, SNU8, ONCOGD1, OVCAR4, and OVCAR3 cell lines were identified as being the most intrinsically sensitive to cisplatin with $GR_{AOC} > 0.6$ and $GR_{50} < 0.5$ μM (Figure 1b). Across the cell line panel, sensitivity to cisplatin (GR_{AOC}) was found to be significantly negatively correlated with sensitivity to cobimetinib (MEK1/2 inhibitor), abemaciclib (CD4/CD6 inhibitor), QL-XII-47 (BTK inhibitor), onalespib (HSP90 inhibitor), ribociclib (PI3K/Akt/mTOR pathway inhibitor), SRA737 (CHK inhibitor) and neratinib (HER1/2/3 inhibitor) (Figure 1c; Spearman $r < -0.30$, p-value < 0.01). Therefore, we hypothesized that cell lines grown to become resistant to cisplatin will become more sensitive to the drugs listed above.

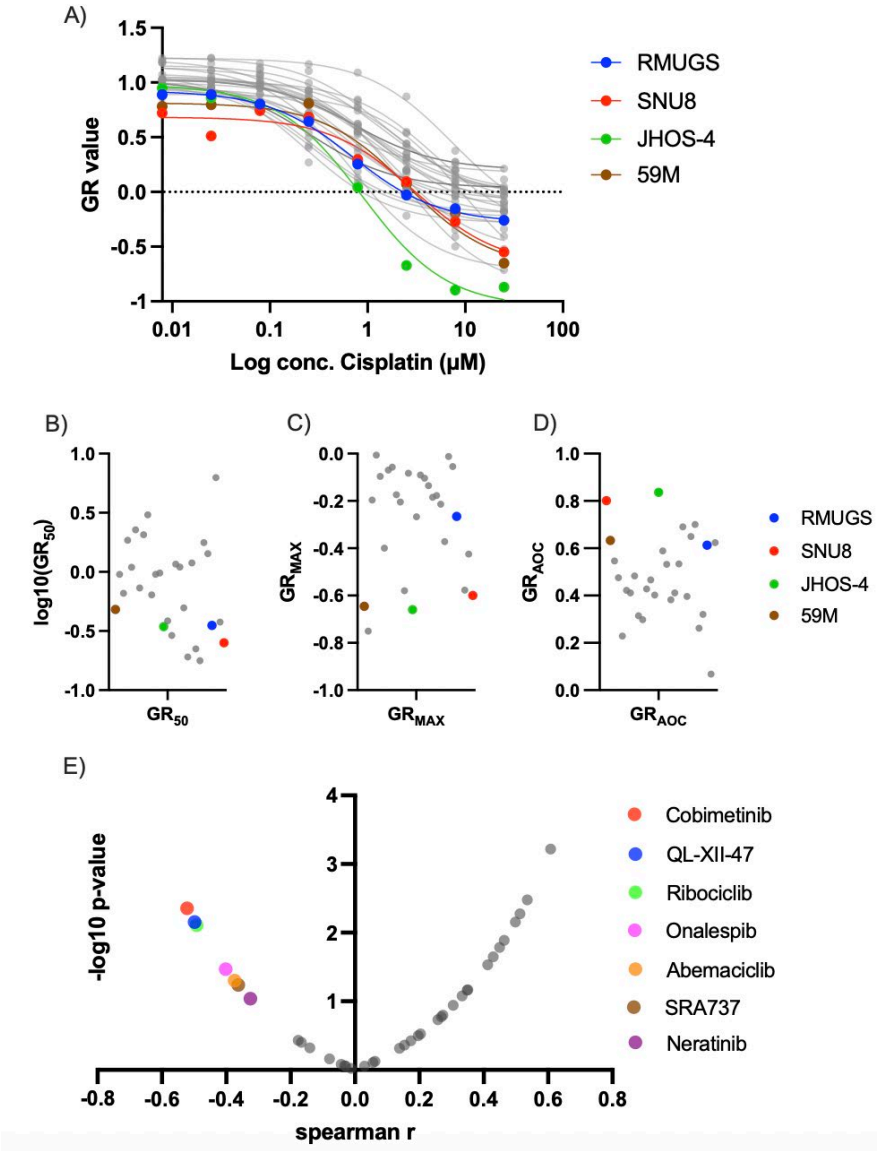

Figure 1. Identification of Cisplatin Resistant Cell Lines and Drug Responses negatively Correlated with Sensitivity to Cisplatin.

Description of Figure 1, (A) Growth rate inhibition (GR) dose response curves for 34 ovarian cancer cell lines treated with 9 doses of cisplatin for 72 h. Nonlinear curve fits are shown. (B) GR_{50}, (C) GR_{max}, and (D) GR_{AOC} metrics corresponding to the curves shown in (A). Cell lines selected for generating cisplatin resistant models are colored (RMUGS in blue, SNU8 in red, JHOS-4 in green and 59M in brown). E) Spearman correlation between the GR_{AOC} of cisplatin and all other drugs in the OvCa-L drug library across 34 ovarian cancer cell lines.

Generation of Cisplatin Resistant Ovarian Cancer Cell Lines

Based on the cisplatin dose response data presented above, four sensitive cell lines (SNU8, RMUGS, JHOS4 and 59M) were selected for the generation of resistant models by long term culture in the presence of increasing concentrations of cisplatin. SNU8 and RMUGS were successfully adapted to sustain proliferation in the presence of 3 μM cisplatin, whereas JHOS4 and 59M did not survive.

To confirm acquired resistance, SNU8 and RMUGS resistant (-PR) and parental (-P) cell lines were treated with a 9-dose half-log dilution series of cisplatin with a maximum dose of 25 μM (Figure 2). For both cell lines, the dose response curves for the parental and PR lines began to separate around 1 μM. At higher concentrations, cisplatin induced negative GR values in the parental lines, indicative of cytotoxicity whereas the response in the PR lines was cytostatic with GR values > 0. The greatest difference between the parental and PR lines was observed at 2.5 μM and 0.8 μM for the SNU8 and RMUGS lines, respectively. Focusing on those concentrations, the mean GR value of SNU8-PR was 3.4-fold higher than SNU8-P ($p=0.048$). The mean GR of RMUGS-PR was 16-fold higher than RMUGS-P although high variability in biological replicates resulted in no significant difference ($p=0.315$) between the RMUGS parental and PR models (Figure 3).

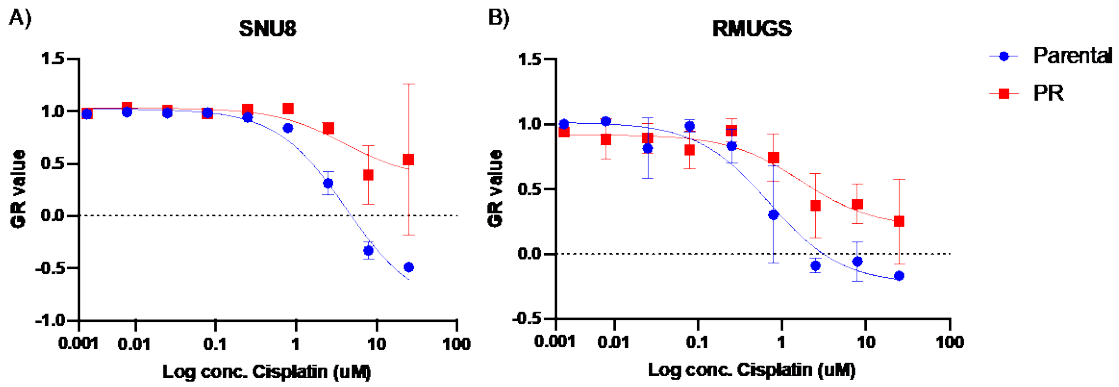

Figure 2. Dose Response of Parental and PR Cell Lines to Cisplatin.

Description of Figure 2, nonlinear regression (curve fit) of concentration of cisplatin versus GR in A) SNU8 and B) RMUGS.

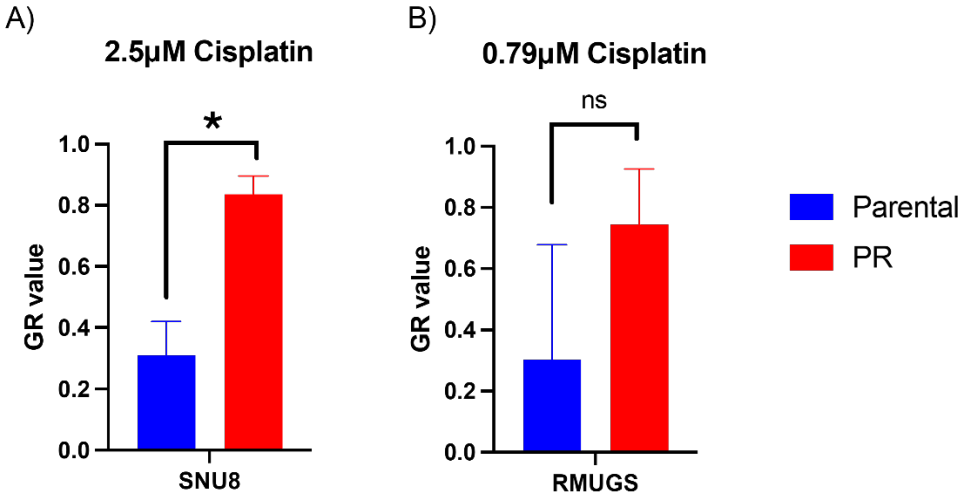

Figure 3. Response of Parental and PR Cell Lines to Cisplatin at Dose of Maximal Effect.

*Description of Figure 3, Bar graph depicting difference in GR between parental and PR cell lines in A) SNU8 at 2.5uM cisplatin and B) RMUGS at 0.79uM cisplatin. Two-way ANOVA mixed effects analysis was used to discern significance (ns, not significant; *, significant).*

Screening Results

To determine if the acquisition of cisplatin resistance changed the sensitivity of the cell lines to other drugs, the parental and PR SNU8 lines were treated with two libraries of small molecule kinase inhibitors. The OvCa-L (33 compounds) and OKL (192 compounds) include FDA-approved drugs currently being used clinically, drugs in clinical trials, as well as novel-preclinical small molecule kinase inhibitors and tool compounds.

Results from the library screens were first evaluated based on which drugs had the strongest overall effect in the resistant model relative to the parental control cells. By quantifying the difference in the area over the GR curves between the PR and parental lines ($GRAOC_{diff}$), we found that the drugs could be categorized into three groups; 1) sensitive, 2) no change, 3) cross resistant. Drugs were classified as "sensitive" if they elicited a stronger effect in the PR model than in the parental control , "no change" if the effect of the drug in the PR model did not differ from its effect in the parental control, or "cross resistant" if the PR model was less sensitive than the parental control. Quantitatively, if the $GRAOC_{diff} \leq -0.20$, the drug was designated cross resistant, and if the $GRAOC_{diff} \geq 0.2$ the drug was assigned to the sensitive group; all other drugs were considered to be equally effective in the parental and PR line (Figure 4A). Of the 225 drugs evaluated, 31 were classified as 'sensitive' and 17 as 'cross-resistant' (Figure 4 B-C) in the SNU8-PR cell line.

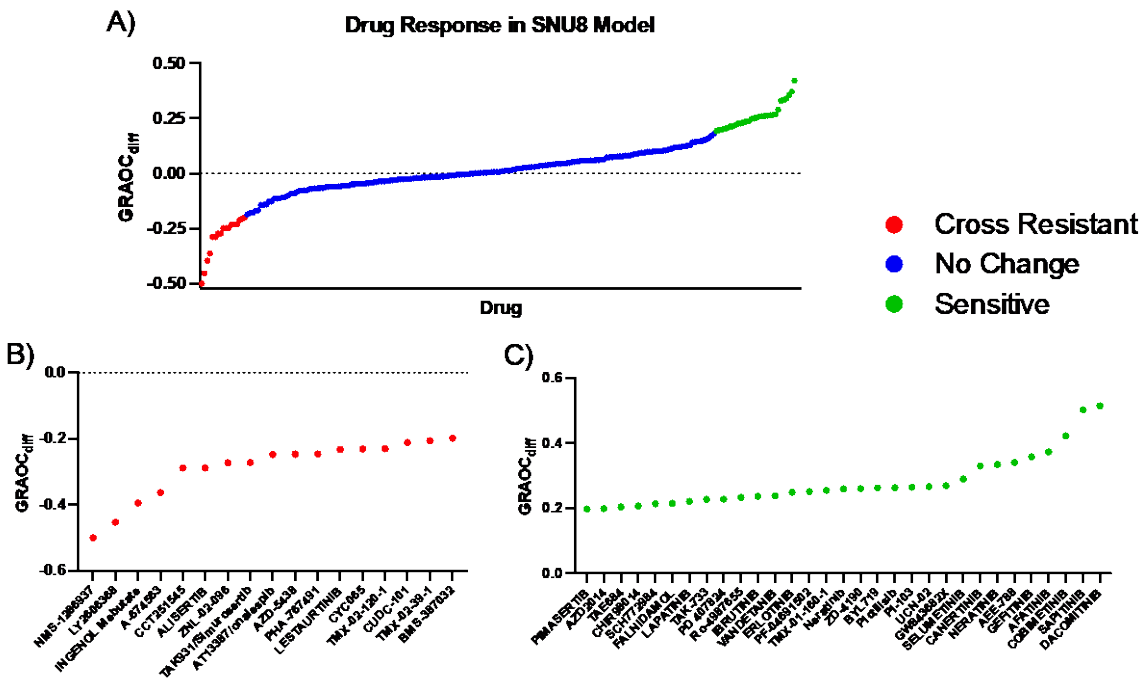

Figure 4. GRAOC Difference Results of Library Screen in SNU8 Model (OKL and OvCa-L).

Description of Figure 4, Results of the screen, $GRAOC_{diff}$ difference of each drug against SNU8-P and -PR are denoted as "Cross Resistant" ($GRAOC_{diff} \leq -0.2$) in red, "No Change" ($-0.2 < GRAOC_{diff} < 0.2$) in blue, and "Sensitive" ($GRAOC_{diff} \geq 0.2$) in green (A). Figure 4B is a focused look at the cross resistant drugs and 4C is a focused look at sensitive drugs. Data from representative replicate (Additional replicates in Appendix, Figure 11-12).

The high degree of variability in RMUGS behavior continued in the screening phase of this work. Although the -PR and parental lines were screened in biological triplicates, only one replicate, in which the cell lines grew well is included here. Compared to the SNU8 cells, the number and magnitude of differential responses between the PR and parental lines was less. For example, across biological triplicates, $GRAOC_{diff}$ responses in the SNU8 model ranged from -1.2 to 1.2, while in the RMUGS

model, the responses from one replicate ranged from -0.43 to 0.28. Therefore, the thresholds for assigning drugs to the "sensitive" and "cross resistant" groups were adjusted: if the $GRAOC_{diff} \leq -0.15$, the drug was designated cross resistant, and if the $GRAOC_{diff} \geq 0.15$ the drug was assigned to the sensitive group; all other drugs were considered to be equally effective in the parental and PR lines (Figure 5A-C). Using these thresholds, the RMUGS-PR line was found to be "cross resistant" to four drugs, and "sensitive" to 15. Overlap between the SNU8 and RMUGS hits were limited to sensitivity to TAE684 (RMUGS $GRAOC_{diff} = 0.18$; and SNU8 $GRAOC_{diff} = 0.20$) and cross-resistance to talazoparib (RMUGS $GRAOC_{diff} = -0.20$; and SNU8 $GRAOC_{diff} = -0.22$). The SNU8 model was prioritized for validation experiments since it was stable throughout the screening phase of the project. Additional screening of the RMUGS model could be performed in the future (see Discussion).

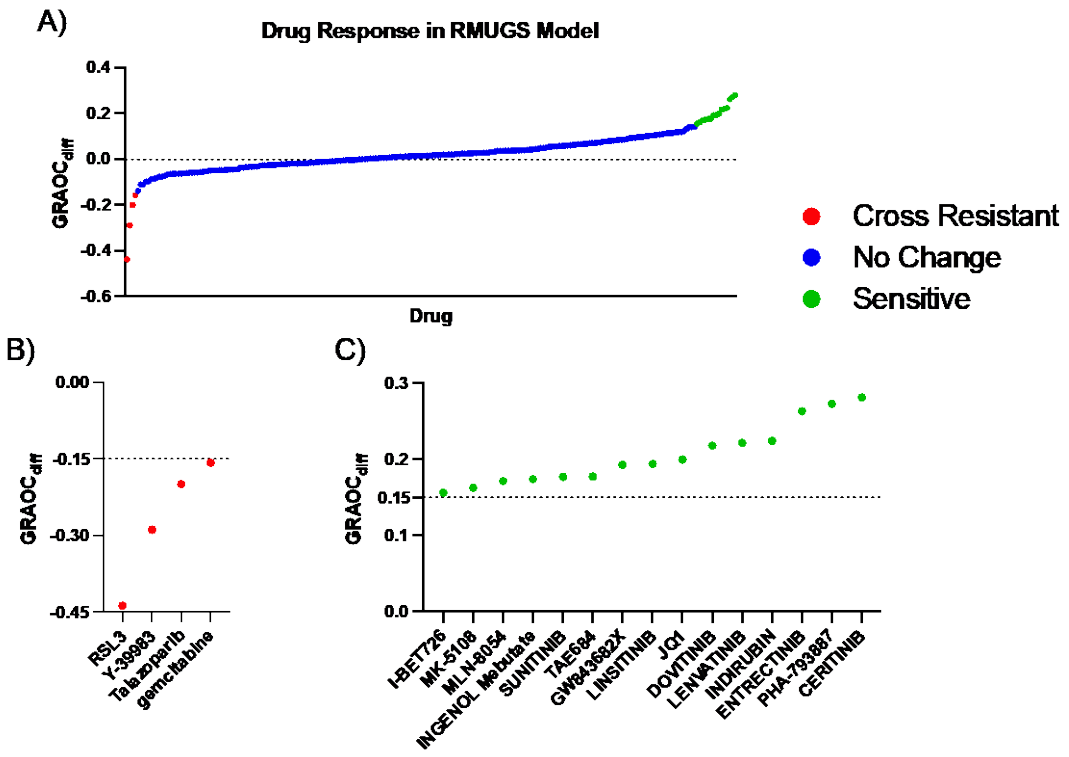

Figure 5. GRAOC Difference Results of Library Screen in RMUGS Model (OKL and OvCa-L).

Description of Figure 5, Results of the screen, $GRAOC_{diff}$ of each drug against RMUGS-P and -PR are denoted as "Cross Resistant" ($GRAOCdiff \leq -0.15$) in red, "No Change" ($-0.15 < GRAOC_{diff} < 0.15$) in blue, and "Sensitive" ($GRAOC_{diff} \geq 0.15$) in green (A). Figure 5B is a focused look at the cross resistant drugs and 5C is a focused look at sensitive drugs.

To narrow down the 31 'sensitive' drug hits for increased effect in the SNU8 PR line, variability among biological and technical replicates was assessed. Drugs with high standard deviation (SD) among biological replicates were flagged. If a high SD was evident across all or most concentrations for a single agent, the given agent was ruled out. Next, the drugs were evaluated based on the magnitude of difference between the PR and parental models. Using $GR_{P\text{-}C}$ at each concentration of the dose response; 17 were found

to have a GR_{P-C} > 0.3 at one or more concentration across biological replicates of the screen. These hits included two out of seven inhibitors found to be negatively correlated with intrinsic sensitivity to cisplatin (cobimetinib and neratinib). Moreover, the cross resistant drugs included TAK931, CYC065 and TMX-02-39-1, three drugs that were positively correlated with cisplatin sensitivity in the profiling data. Taken together, these results suggest that there may be shared mechanisms behind intrinsic and acquired cisplatin resistance.

To further narrow down the hits, inhibitory effects across concentrations, activity at lower doses, redundancy in target coverage and clinical status were considered. Drugs exhibiting an inhibitory effect at lower concentrations were prioritized while drugs that only showed an effect at the highest dose (10 μM) were de-prioritized. Additionally, results were compared across biological replicates to verify consistency and reproducibility in the data and rule out any outliers (Table 2).

Table 2. GR_{P-C} over 0.3 of Top Hits.

	GR_{P-C}			
	0.01 μM	0.1 μM	1 μM	10 μM
AEE-788			0.58	0.68
Afatinib	**0.29**	**0.48**	**0.62**	
Alpelisib		**0.38**	**0.41**	
Canertinib		0.29	0.60	
Cobimetinib				**0.42**
Dacomitinib		**0.45**	**0.56**	**0.54**
Erlotinib			**0.33**	**0.49**
Falnidamol			0.46	
Pictilisib		**0.38**	**0.43**	
Gefitinib			0.61	
Ibrutinib			**0.49**	**0.49**
Neratinib		0.64	0.62	0.47

	GR_{P-C}			
	0.01 μM	0.1 μM	1 μM	10 μM
PF-04691502		0.55	0.30	
Sapitinib		0.41	0.61	0.49
TAE684				**0.45**
UCN-02		0.33		
ZD-4190			0.50	0.38

Table 2 shows the geometric mean of ratios across triplicates of GR_{P-C} values over 0.3 for top hits in SNU8 cell line model at four doses.

KINOMEscan data was used to evaluate target coverage by the hits. Kinase inhibitors often hit kinases other than their intended target, and these kinases can contribute to effects in cells (Anastassiadis et al., 2011). Therefore, KINOMEscan data for the 17 top hits were analyzed to identify common targets and help narrow down inhibitors of interest for follow-up experiments. The KINOMEscan assay measures the percent inhibition of a drug against 468 kinase targets; a value of 100% means the drug does not inhibit that kinase and a value of 0% means the drug fully inhibits that kinase at the concentration tested (Fabian et al., 2005). In this case, 100 nM was used for screening to identify kinases inhibited at low doses (Figure 6).

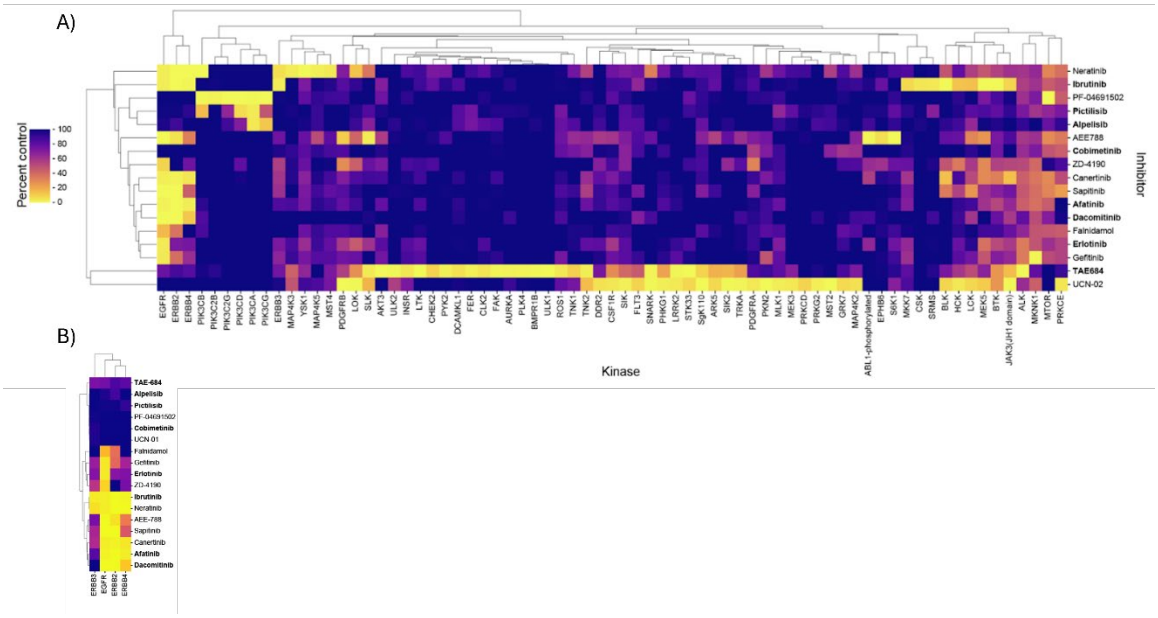

Figure 6. Hierarchical clustering of KINOMEscan percent control values at 100 nM for the top 17 compounds.

Description of Figure 6, (A) All kinases that were inhibited to 10% of control or less by at least one inhibitor are shown. The inhibitors that were used in subsequent experiments are in bold. (B) The same data as in (A) showing only the EGFR family kinases for the 17 hit compounds.

The EGFR family was strongly inhibited by 11/17 of the hits: with two pan-ERBB inhibitors, five that spare ERBB3 but that are otherwise potent inhibitors of EGFR, ERBB2 and ERBB4, and four specific EGFR inhibitors (Figure 6, Table 3). At least one drug covering each scenario was selected for validation experiments based on clinical status and performance in the screen. Since neratinib was included in both the LINCS-OVCA and OKL libraries and hit from screening both, ibrutinib was selected as the pan-ERBB inhibitor to move forward into validation testing. Ibrutinib's off-targets also differ from those of neratinib, leading to the hypothesis that they are both effective in

the PR setting due to their shared on-target pan-ERBB activity. Erlotinib was selected as the selective EGFR inhibitor and, the ERBB3-sparing inhibitors, Afatinib, and Dacomitinib were selected for further testing. TAE684 and UCN-02 both exhibited multi-targeting inhibition of kinases with no ERBB activity, TAE684 was included in the validation experiments because it was the only agent to also elicit sensitivity in the RMUGS model. Additional hits included PI3K inhibitors; alpelisib (PI3Ka specific), and pictilisib (PI3Kb-sparing) were selected for further evaluation as well as cobimetinib, the only hit to target MEK (Table 3).

Table 3. Kinome Scan Data Summary of Top 17 Drug Hits.

	Clinical Status	Target(s)
Falnidamol	Phase 1	EGFR
Gefitinib	Approved	EGFR
ZD-4190	tool	EGFR
Erlotinib	**Approved**	**EGFR**
AEE-788	Phase 1/2	EGFR, ERBB 2,4
Afatinib	**Approved**	**EGFR, ERBB 2,4**
Canertinib	Phase 2	EGFR, ERBB 2,4
Dacomitinib	**Approved**	**EGFR, ERBB 2,4**
Sapitinib	Phase 2	EGFR, ERBB 2,4
Neratinib	Approved	pan ERBB
Ibrutinib	**Approved**	**pan ERBB + off targets**
TAE684	**tool**	**multi targeting, no ERBB activity**
UCN-02	tool	multi targeting, no ERBB activity
Cobimetinib	**Approved**	**MEK**
Alpelisib	**Approved**	**PIK3CA specific**
Pictilisib	**Phase 2**	**Pan PI3K**
PF-04691502	Phase 2	pan PI3K + mTOR

Table 3 includes the top 17 drug hits, clinical status and summary of target inhibition from the KINOMEscan data. Bolded rows indicate drugs moved forward into the validation experiment.

Validation Results

Each of the hits identified above was re-tested in 9-point dose responses in the SNU8-P and -PR cell lines. All hits except TAE-684 and ibrutinib showed increased inhibition in the -PR model (Figure 7). When looking at GR metrics, there is an overall increase in GRAOC and decrease in GRmax in the PR line compared to the parental line. Although, dacomitinib was the only drug to elicit a significant difference in GRmax ($p=0.0264$) while both dacomitinib and alpelisib showed a significant difference in GR_{AOC} with p-values of 0.0443 and 0.0043, respectively (Figure 8). These results could be due in part to variability between biological replicates. When evaluating the $GRAOC_{diff}$, the magnitude of difference between parental and PR between the replicates was generally consistent (Table 4).

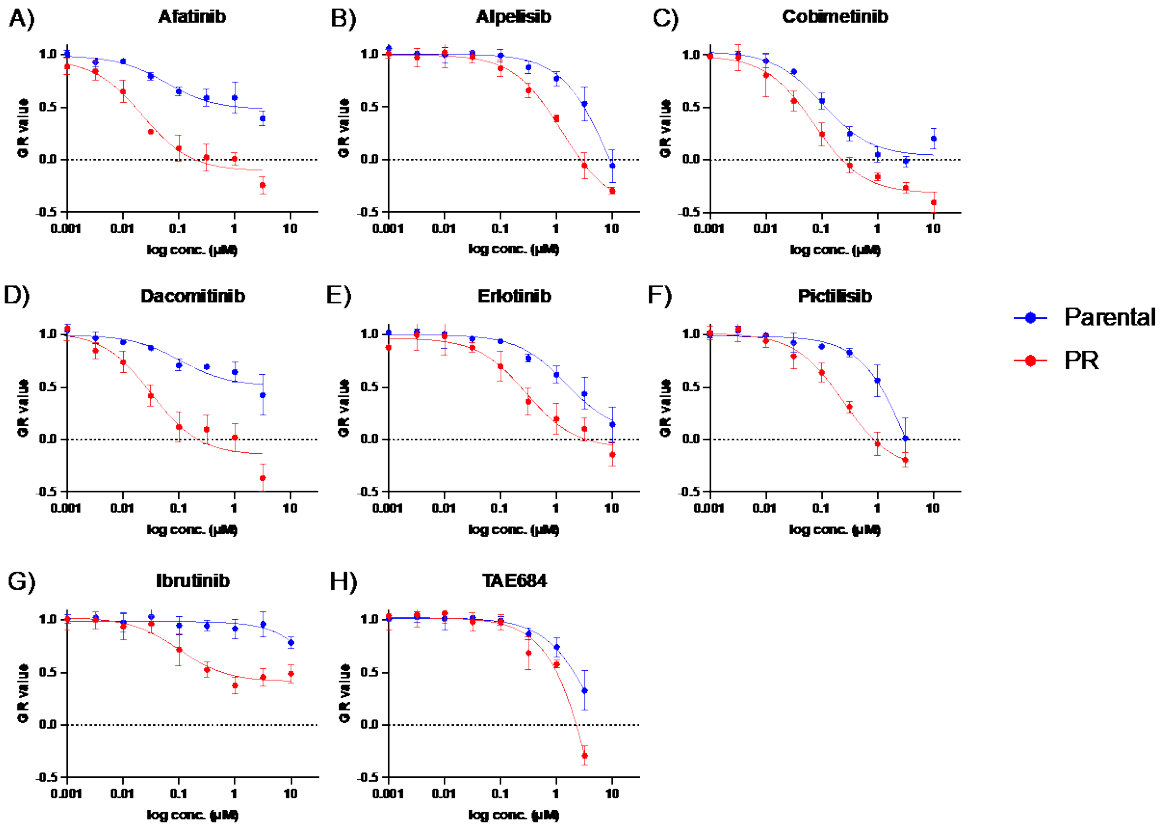

Figure 7. Dose Response of Parental and PR Cell Lines in Response to Top 8 Drug Hits.

Description of Figure 7, nonlinear regression (curve fit) of concentration of A) afatinib, B) alpelisib, C) cobimetinib, D) dacomitinib, E) erlotinib, F) pictilisib, G) ibrutinib and H) TAE684 versus GR response of SNU8-P (blue) and SNU8-PR (red). . Data from representative replicate (Additional replicate in Appendix Figure 13).

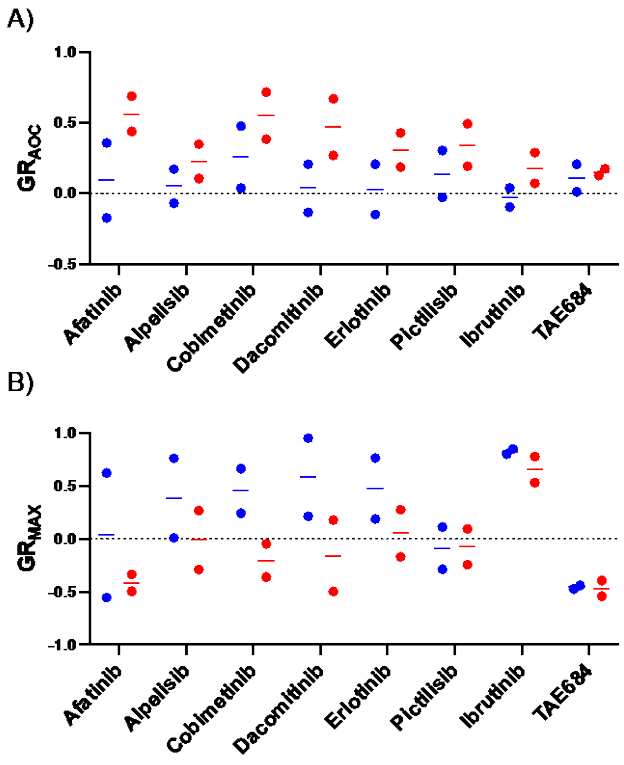

Figure 8. GR Metrics Summary of Validation Experiments.

Description of Figure 8, mean GR_{AOC} (A), GR_{50} (B), and GR_{max} (C) values of validation experiments (duplicates) with Parental in blue and PR in red.

Table 4: Difference in GR_{AOC} of biological replicates.

	$GRAOC_{diff}$	
	(a)	(b)
Afatinib	0.331	0.611
BYL719	0.177	0.174
Cobimetinib	0.240	0.347
Dacomitinib	0.464	0.403
Erlotinib	0.222	0.337
GDC-0941	0.189	0.221
Ibrutinib	0.250	0.166
TAE684	-0.031	0.116

Table 4 shows the difference in GR_{AOC} ($GRAOC_{diff}$) of biological replicates from the validation experiment.

RNA sequencing was performed to investigate possible molecular changes to the resistant cells that could explain their increased sensitivity to the validated hits (Figure 9). Further analysis of the significantly up- or down-regulated genes (Figure 10) highlighted an increase in KRAS signaling in SNU8 which can lead to constitutive activation of MAPK. This can in part explain the increased sensitivity to EGFR and MEK inhibition via their upstream and downstream inhibition of KRAS, respectively.

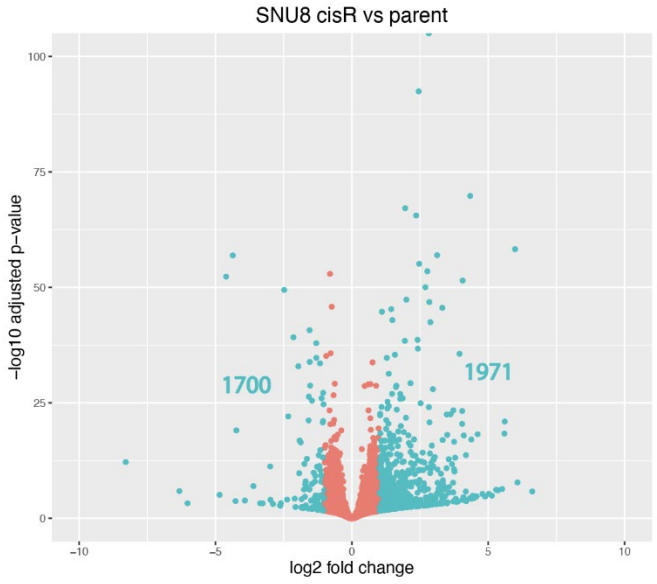

Figure 9. Number of significantly up- or down-regulated genes (adjusted p-value < 0.05).

Description of Figure 9, volcano plots depicting the number of significantly up- and down-regulated genes (PR:parental). Blue indicates significant and red indicates not significant up or down regulation.

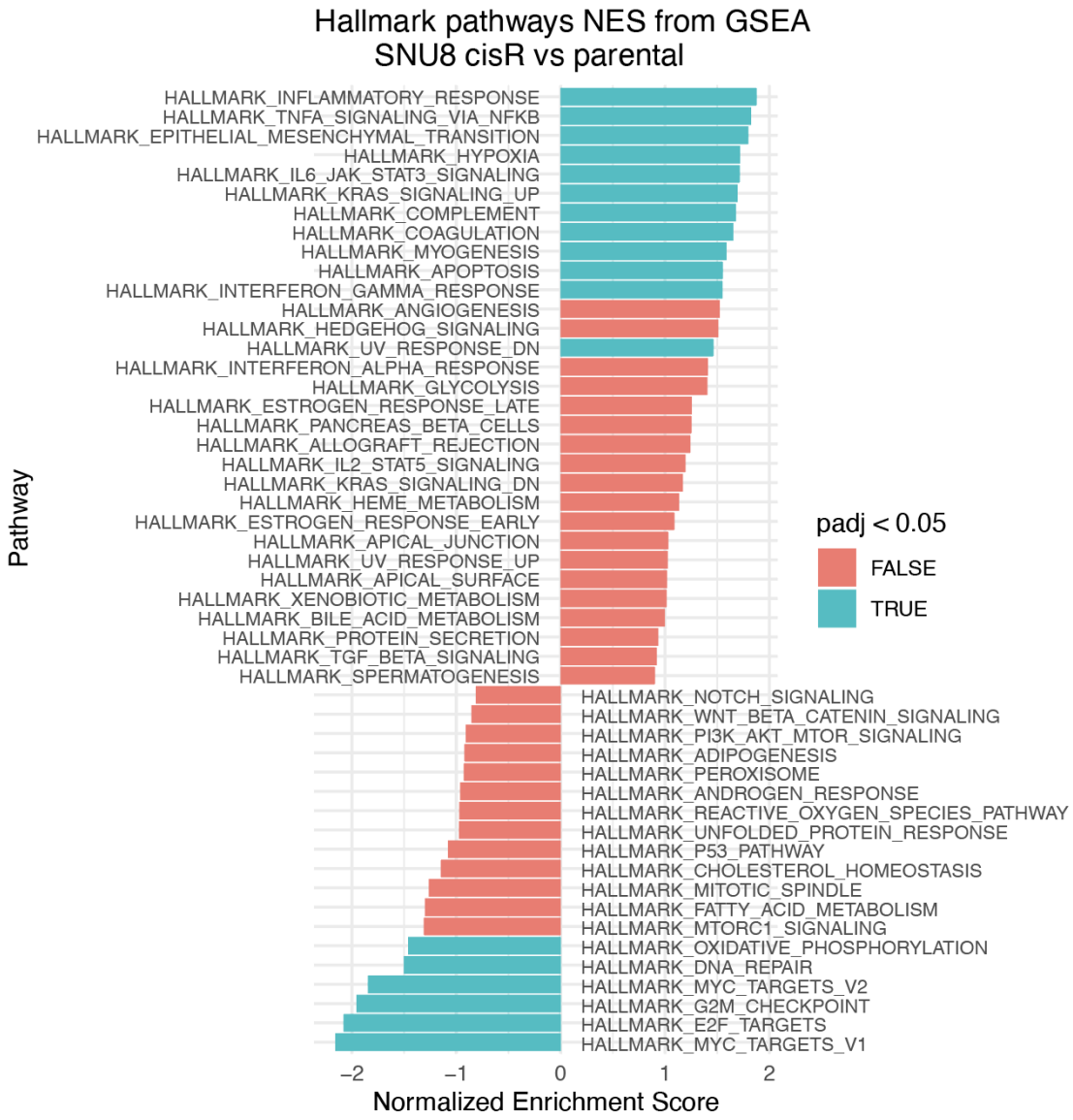

Figure 10.Normalized enrichment scores (NES) for the Hallmark pathways from Gene Set Enrichment Analysis (GSEA).

Description of Figure 10, Bar plots depicting results NES scores from a GSEA for gene lists in Figure 9, with genes ranked according to p-value for SNU8.

Chapter IV.

Discussion

Based on published research and our own dose response studies, it was hypothesized that EGFR, PI3K/Akt/mTOR, and PARP pathway inhibitors would prove efficacious in combatting PR in HGSOC (Peng et al., 2010; Poursheikhani et al., 2020; J. Zhang et al., 2013). In the work presented in this thesis, PARP inhibition was not found to be effective in an acquired PR cell line model compared to parental control. However, in a screen of small molecule drugs covering most of the kinome, selective EGFR, PI3K and MEK inhibitors showed significantly greater effects in PR cells than in parental controls. Together, these data agree with previous research on the potential efficacy of PI3K and EGFR inhibitors in PR HGSOC and identifies MEK as a pathway of interest for further investigation.

Significance

PR Cell Line Model Implications

When evaluating PR in HGSOC in previous research, the most common cell line models used in vitro were SKOV3 and A2780 (Domcke et al., 2013). Recently, a comprehensive analysis of genomic data and molecular profiles of HGSOC cell lines and tumor tissues was conducted to identify the best cell line models for in vitro experiments and identify cell lines that are inaccurate models of HGSOC tumors. The originators of SKOV3 and A2780 cell lines did not assign them a histological subtype but both are widely used in the literature as HGSOC models. However, based on their molecular

profiles and genetic mutations, SKOV3 and A2780 are most likely not HGSOC (Domcke et al., 2013). Additionally, of 5,693 publications included in the study, SKOV3 and A2780 cell lines accounted for 60% of the research conducted in HGSOC, highlighting how widely used they have been (Domcke et al., 2013). For example, all of the research discussed in the introduction to this thesis on EGFR and PI3K/Akt/mTOR inhibitors in HGSOC was conducted in SKOV3, A2780 and in one case, IGROV1 which was also identified as a poor HGSOC model due to the cell line being hyper mutated (Cai et al., 2014; Deng et al., 2019; Liu et al., 2015; Michels et al., 2013; Sima et al., 2018; S. Wang et al., 2015; Xu et al., 2021; Yang et al., 2020; J. Zhang et al., 2013). In our OvCa profiling project, we found SKOV3 cells to be intrinsically resistant to cisplatin (GRAOC ~0.15). Therefore, we leveraged data from the OvCa profiling project to select cell lines that were intrinsically sensitive to cisplatin and, confirmed as accurate HGSOC models based on their genomic data and molecular profiles as the starting point for generating relevant PR cell line models.

Furthermore, while IC_{50}, E_{max} and AOC calculations are widely used in pharmacology research, the results can be skewed when comparing cell lines with different proliferation rates (Hafner et al., 2016). Such differences in baseline growth rates can result in dramatic variations of IC_{50} and Emax values and have the potential to lead to skewed data comparisons and inaccurate conclusions. GR metrics account for cell proliferation and normalize the drug inhibitory effects to the effect in a single population doubling. Thus evaluating the efficacy of drugs in terms of GR inhibition is a more accurate measurement of relative sensitivity and should be used when comparing preclinical data from differing cell lines to increase the translational potential of results

(Hafner et al., 2016). The use of GR metrics was important in this work for the initial identification of cisplatin-sensitive cell lines, and then for comparisons between the parental and induced PR models since the PR lines generally grew more slowly than the parents.

The process of generating the PR models involved continuous exposure to cisplatin in the growth media starting at 0.5 μM. While the SNU8 cell line was the second most intrinsically sensitive to cisplatin (JHOS-4 being the most sensitive), it was the only cell line able to adapt and consistently proliferate in the presence of 3 μM cisplatin. JHOS-4 cells were never able to proliferate in cisplatin-containing media; they were just too sensitive with a GR_{50} of 17 nM compared to 480 nM, 350 nM, and 250 nM in 59M, RMUGS, and SNU8, respectively. Although RMUGS and 59M PR cell line models were generated, they were inconsistent (see Limitations), thus the SNU8 cell line provided the most robust model to move forward with. By using a PR-parental paired model of SNU8 for screening, the data collected allows for a direct evaluation of changes induced as a consequence of acquired cisplatin resistance.

Implications of Screening and Validation Results

The initial screen in the SNU8 PR-model consisted of 225 small molecule kinase inhibitors including FDA-approved drugs currently being used clinically, drugs in clinical trials, novel-preclinical small molecule kinase inhibitors and established tool compounds. Most of the drugs have been profiled to measure their binding affinities to over 400 kinases using the KINOMEscan SCANmax platform from Eurofins. These data were leveraged to assess the target coverage and selectivity of drugs of interest to provide additional insight on the results of the screen and the validation experiment. In particular,

the KINOMEscan results provided confidence in attributing drug effects to specific targets.

Multiple drugs previously reported to be effective in preclinical PR studies (see introduction) were also evaluated in the initial screen. Previously, CUDC-101 (EGFR inhibitor) and PI-103 (PI3K inhibitor) were reported to resensitize PR A2780 and SKOV3 cell line models, respectively, to cisplatin (Cai et al., 2014; Sima et al., 2018). While the goal of this thesis was to identify vulnerabilities in PR cells rather than to re-sensitize them to cisplatin, in the initial screen, the PR model was more sensitive to PI-103 ($GRAOC_{diff}$ of 0.26) but cross resistant to CUDC-101 ($GRAOC_{diff}$ of -0.21). Based on KINOMEscan data, CUDC-101 also has pan HDAC activity. This pathway has been investigated and, when inhibited, shown to re-sensitize cells to cisplatin therefore, this agent may be best suited to that application rather than as an alternative single agent therapeutic for treating cisplatin resistance (Rodrigues Moita et al., 2020). In addition to the possibility that the benefits of CUDC-101 in the PR setting are limited to co-treatment with cisplatin, it is also possible that the conflicting CUDC-101 results are due to cell-line specific differences (A2780 which is a poor model of HGSOC vs SNU8) (Domcke et al., 2013).

It was clear from the KINOMEscan data that many of the top hits found to have greater effects in PR cells compared to parental cells were selective EGFR family inhibitors with minimal to no kinase off-targets. The highly selective and FDA-approved EGFR inhibitors, afatinib, dacomitinib and erlotinib were more effective in the SNU8-PR cells than the parental cells. Validation of their enhanced effect in the PR setting coupled with the finding that the multi-targeting, but EGFR-family sparing, inhibitor TAE684 that

was also an initial screening hit, did not elicit a significant difference in response between the parental and PR cell line models in follow-up experiments suggest that EGFR inhibition is a key vulnerability in PR HGSOC. The pan-EGFR family inhibitor, ibrutinib, did not validate in follow-up experiments; however, we note that it is not as selective as the others, and it is possible that inhibition of its additional targets results in similar effects in the PR and parental models. When we looked at the KINOMEscan data for the cross-resistant hits, there was no obvious group of commonly inhibited kinases.

Drug hits were selected for further evaluation in the validation experiment based on consistency of results, magnitude of $GRAOC_{diff}$, inhibition at lower doses (GR_{P-C}), and KINOMEscan data. Both alpelisib and pictilisib were selected for validation studies because they selectively inhibit PI3K and have no off-target binding affinity for EGFR, making these PI3K inhibitors ideal candidates to evaluate the efficacy of specifically targeting the PI3K/AKT/mTOR pathway to treat PR-HGSOC. The observation that sensitivity to alpelisib across the 34 cell lines in the OvCa profiling project was negatively correlated with sensitivity to cisplatin could be an indicator of a shared vulnerability between intrinsic PR and the acquired PR model. Since alpelisib is already FDA-approved to treat metastatic breast cancer, the regulatory process to add it to treatment options for ovarian cancer would be easier than for a drug that is still in preclinical development (Singh et al., 2024). In addition to alpelisib, pictilisib (a PI3Kb-sparing inhibitor) was also a hit and both compounds increased cell death in the PR model in validation experiments. This finding suggests that EGFR inhibition is not the only druggable vulnerability in PR cells.

Lastly, cobimetinib (MEK1/2 inhibitor) was evaluated in the validation experiments since it was a strong screening hit and responses to cobimetinib and cisplatin were negatively correlated in the OvCa profiling project. In follow-up experiments, cobimetinib elicited a significantly stronger response in the PR model compared to the parental cells, with an average 2-fold increase in GRAOC, from 0.25 to 0.55 for parental and PR, respectively. MEK inhibitors have proven successful in other cancer types and trametinib, also a MEK inhibitor, has been approved by the FDA for treatment of BRAF V600E mutated metastatic non-small cell lung cancer (Odogwu et al., 2018) and more recently for low grade serous ovarian cancer, proving more efficacious in comparison to the standard of care (Gershenson et al., 2019). While the MEK pathway has not been heavily researched in the treatment of PR HGSOC, one study found that MAPK activation played a role in PR ovarian cancer and a MAPK inhibitor in combination with a microRNA targeting RNF2 down regulation resulted in decreased cell viability (Chen et al., 2018).

PARP inhibitors have been previously investigated for the treatment of PR OVCA or as a tool to resensitize PR models to cisplatin and the PARP inhibitor, olaparib is approved by the FDA for the treatment of ovarian cancer (Vanderstichele et al., 2019). In the OvCa profiling project, olaparib sensitivity was negatively correlated with cisplatin sensitivity leading to the hypothesis that PARP inhibition could be a vulnerability in PR. However, in the initial screen of SNU8-PR and parental cells, olaparib did not elicit a differential effect between the lines ($GRAOC_{diff}$ of 0.044), and the PR model was found to be cross resistant to talazoparib ($GRAOC_{diff}$ of -0.178) (Murai et al., 2014). As previously discussed, if PR is the result of aberrant NER or if mutations leading to HR-

proficiency have occurred, PARP inhibitors would not be as effective based on their mechanism of action (Konstantinopoulos et al., 2015). Previous research has described PR to cisplatin to be caused by NER repair of cisplatin-induced DNA damage and is one rationale as to why PARP inhibitors were not efficacious in the screen (Duan et al., 2020). Additionally, RNA sequencing results from the data presented in this thesis showed downregulation of DNA repair which could be yet another reason why response to PARP inhibition is not seen in the PR model. The data presented here do not support blanket use of PARP inhibitors in the treatment of PR HGSOC but rather highlight possible differences between intrinsic and acquired resistance as well as the need for additional models of acquired PR.

Limitations

In the generation of PR cell lines derived from cell lines intrinsically sensitive to cisplatin, only one cell line proved to be a robust model. JHOS-4 was unable to proliferate at the lowest concentration of cisplatin tested (0.5 μM), and while the 59M and RMUGS lines were adapted to grow in cisplatin, the 59M-PR results were inconsistent, and the RMUGS-PR proliferative capacity slowed over time. In these experiments, the concentrations of cisplatin were predefined and kept consistent across all cell lines; it may have been better to use GR_{50} values to inform the optimal starting concentration of cisplatin and increase cisplatin concentration in a dose dependent manner from there (Barr et al., 2013). It is also possible that allowing the cells more time to adapt to each concentration of cisplatin would have yielded more consistent results in the cell line models which failed (Barr et al., 2013). This is the largest limitation of the study, and further hypothesis testing and investigation of results that conflict with

previously published data will require additional models which could include those that were initiated in this study but were not robust enough in time for screening.

The initial screen of the Optimal Kinase Library only consisted of 4 dose points for each drug and therefore limited the resolution of the extracted GR metrics . While a 9-point dose response structure would have been optimal, the time, cost and resources needed for an experiment of this size meant that it was not feasible. Because of this, experiments to validate the top hits from the screen were performed over 9-dose points.

Future Directions

In previous research and in the work performed in this thesis, EGFR inhibitors proved efficacious in combatting PR and inducing cell death. However, in the clinic, both gefitinib and erlotinib have failed in the treatment of PR HGSOC although, EGFR overexpression was not a criterion for enrollment in the trials (Siwak et al., 2010; Wilken et al., 2012). It is possible that EGFR inhibitors could be beneficial with more personalized treatment strategies. Future research would benefit from exploring EGFR overexpression as a biomarker in predicting patient response and as a criterion to be used in clinical trials. Additional work to bridge the gap between cell line models of PR and the clinical experience is warranted. A first step extending from the results in this thesis would be to xenograft the SNU8-PR cells in mice and treat them with EGFR inhibitors. This would help to elucidate where the breakdown in translation from bench to clinic occurs.

In addition to moving towards in vivo validation in animals, there are several next steps that could be taken in cell lines. It would prove advantageous to work on stabilizing the other cell lines tested here to be durable PR cell line models. Specifically, 59M and

RMUGS could become stable models by providing them more time between cisplatin dose increases as well as increasing the dose in smaller increments. Additionally, instead of starting all cell lines at one dose of cisplatin, each could be started doses based on their GR_{50}'s from the ovarian cancer profiling results.

Another direction to expand on these results would be investigating the effects of the top hits in combination with cisplatin. Several published studies are focused on resensitizing cells to cisplatin, and combination studies with simultaneous drug treatments or experiments in which PR cells are pretreated with the targeted hit compounds followed by treatment with cisplatin would allow for more direct comparisons to existing literature. Although there is an abundance of preclinical evidence outlining the importance of the PI3K/Akt/mTOR pathway in EOC, targeting it in clinical trials has been poorly tolerated and led to failure. Previous research suggests that inhibitors targeting the PI3K/Akt/mTOR pathway would be best used in combination with cisplatin which would allow for both therapies to be administered at lower concentrations, ideally decreasing the risk of adverse side effects in patients (Cai et al., 2014; Deng et al., 2019; Liu et al., 2015).

Interestingly, it has been reported, specifically in EGFR/HER2 driven cancers, that inhibition of the MEK pathway drives hyperactivation of HER3 (ERBB3) and that through a feedback loop, it can lead to PI3K/Akt activation (Turke et al., 2012). Additionally, research of MEK inhibition in ovarian cancer has mostly been in the context of a combination treatment. Taking together previous research on MEK inhibition and data from the screen and validation experiments performed here, it would be advantageous to investigate multiple drug combinations from the top hits of the screen.

First, cobimetinib which is a highly selective MEK inhibitor, in combination with Afatinib which is a pan EGFR inhibitor highly selective for HER3, would be one avenue to investigate if MEK and HER3 inhibition in combination could prove successful in the context of PR HGSOC. Second, cobimetinib in combination with pictilisib or alpelisib could provide contextually relevant data on the efficacy of inhibiting both the MEK and PI3K/Akt pathway. Additionally, based on upregulation of the inflammatory response pathway in the PR model, testing the efficacy of the top drug hits in combination with immune therapy such as anti-PD-1, could prove to be an further combination treatment strategy for PR HGSOC (H. Zhang et al., 2020).

Lastly, performing deeper analysis of the RNA sequencing data could elucidate patterns not yet recognized. Aside from drawing conclusions based off of the up- and down-regulated pathways themselves, taking an in-depth approach to analyzing what genes are in each of those pathways and if there is a commonality could provide insight into important targets to pursue in future research.

Appendix

Table 5. Agents in the OvCa-L and OKL drug libraries.

Library	Agent
OvCa-L (33)	Onalespib
	AZD1775
	AZD2014
	Olaparib
	AZD5363
	AZD6738
	Abemaciclib
	BYL719
	CYC065
	Cobimetinib
	Pictilisib
	LY2606368
	LY3023414
	Neratinib
	PF-06873600
	QL-VIII-58
	QL-X-138
	QL-XII-47
	RSL3
	Ribociclib
	SRA737/CCT245737
	SY-1365
	Simurosertib
	TMX-01-160-1
	TMX-02-120-1
	TMX-02-39-1
	Talazoparib
	Torin1
	Torin2
	Berzosertib
	YKL-5-124
	ZNL-02-096
	ZXH-5-168-145
OKL	A 1070722

Library	Agent
OKL	A-674563
	AEE-788
	AFATINIB
	ALECTINIB
	ALISERTIB
	ALSTERPAULLONE
	ALVOCIDIB
	AMG-208
	AMG-548
	APITOLISIB
	AST-487
	AT-7519
	AT-9283
	AXITINIB
	AZAKENPAULLONE
	AZD-1480
	AZD-5438
	AZD-8055
	BARASERTIB
	BARICITINIB
	BAY61-3606
	BGJ398
	BI-2536
	BIX 02565
	BMS-345541
	BMS-387032
	BMS-509744
	BMS-599626
	BMS-754807
	BMS-777607
	BMS-911543
	BOSUTINIB
	BRIVANIB
	Barasertib-HQPA
	CABOZANTINIB
	CANERTINIB
	CAY10561
	CCT251545
	CEDIRANIB
	CEP-1347
	CERITINIB
	CHIR98014

Library	Agent
OKL	COBIMETINIB
	CP-724714
	CRIZOTINIB
	CUDC-101
	CYC-116
	DABRAFENIB
	DACOMITINIB
	DACTOLISIB
	DANUSERTIB
	DASATINIB
	DB07268
	DORAMAPIMOD
	DOVITINIB
	ENMD-2076
	ENTRECTINIB
	ENZASTAURIN
	ERLOTINIB
	FALNIDAMOL
	FASUDIL
	FEDRATINIB
	FORETINIB
	GALUNISERTIB
	GDC-0879
	GDC-0994
	GEDATOLISIB
	GEFITINIB
	GNE-3511
	GSK-1070916
	GSK-269962A
	GSK-319347A
	GSK-690693
	GSK1838705A
	GSK1904529A
	GSK2334470
	GSK2606414
	GW632580X
	GW843682X
	H-1152
	HARMINE
	I-BET726
	IBRUTINIB
	IMATINIB

Library	Agent
OKL	INDIRUBIN
	INGENOL Mebutate
	IPATASERTIB
	JNJ-28312141
	JNJ-38877605
	JNJ-7706621
	JQ1
	KW-2449
	LAPATINIB
	LENVATINIB
	LESTAURTINIB
	LINIFANIB
	LINSITINIB
	LOSMAPIMOD
	LY-2090314
	MGCD-265A
	MIDOSTAURIN
	MK-2206
	MK-5108
	MK2 inhibitor III
	MLN-8054
	MLN120B
	MOMELOTINIB
	MOTESANIB
	NERATINIB
	NILOTINIB
	NINTEDANIB
	NMS-1286937
	NVP-TAE226
	ORANTINIB
	OSI-632
	OSI-930
	PACLITAXEL
	PALBOCICLIB
	PAMAPIMOD
	PAZOPANIB
	PD 407824
	PD-0325901
	PD173955
	PD184352
	PELITINIB
	PF-04217903

Library	Agent
OKL	PF-04691502
	PF-3758309
	PF-562271
	PFI-1
	PH-797804
	PHA-767491
	PHA-793887
	PI-103
	PIM-447
	PIMASERTIB
	PONATINIB
	QUIZARTINIB
	R-1487
	RAF 265
	REBASTINIB
	RG-1530
	RG-547
	RK-24466
	ROCILETINIB
	RUBOXISTAURIN
	RUXOLITINIB
	Ribociclib
	Ro-4987655
	SAPITINIB
	SARACATINIB
	SB-203580
	SB-431542
	SB772077
	SCH772984
	SELICICLIB
	SELUMETINIB
	SGI-1776
	SGX-523
	SILMITASERTIB
	SNS-314
	SORAFENIB
	SOTRASTAURIN
	STAUROSPORINE
	SU-014813
	SUNITINIB
	TAE684
	TAK-285

Library	Agent
	TAK-593
	TAK-715
	TAK-733
	TALMAPIMOD
	TAMATINIB
	TANDUTINIB
	TANZISERTIB
	TCS JNK 6o
	TELATINIB
	TIVOZANIB
	TOFACITINIB
OKL	TORIN1
	TOZASERTIB
	Tepotinib
	Tilfrinib
	UCN-02
	VANDETANIB
	VATALANIB
	VEMURAFENIB
	VX-745
	Y-27632
	Y-39983
	ZD-4190

Table 5 consists of all drugs included in the OvCa-L and OKL libraries used in the screening assay.

Table 6. Summary of GRAOCdiff across replicates in SNU8 Model

Agent	$GRAOC_{diff}$			Average $GRAOC_{diff}$
	(a)	(b)	(c)	
GEFITINIB	0.27	0.65	0.36	0.43
DACOMITINIB	0.33	0.41	0.51	0.42
PF-04691502	0.17	0.71	0.25	0.38
IBRUTINIB	0.23	0.63	0.24	0.37
SAPITINIB	0.41	0.08	0.50	0.33
AEE-788	0.22	0.41	0.34	0.32
AFATINIB	0.14	0.36	0.37	0.29
NERATINIB	0.16	0.36	0.33	0.28
CANERTINIB	-0.02	0.52	0.33	0.28
ERLOTINIB	0.17	0.34	0.25	0.25

Agent	GRAOCdiff			Average $GRAOC_{diff}$
	(a)	(b)	(c)	
FALNIDAMOL	0.18	0.34	0.21	0.25
GDC-0941	0.13	0.30	0.26	0.23
COBIMETINIB	0.03	0.14	0.42	0.20
BYL719	0.09	0.22	0.26	0.19
TAE684	0.09	0.10	0.20	0.13
UCN-02	0.13	-0.01	0.27	0.13

Table 6 shows the top 17 drug hits average $GRAOC_{diff}$ across all replicates (a though c) and the average of the replicates in the far-right column.

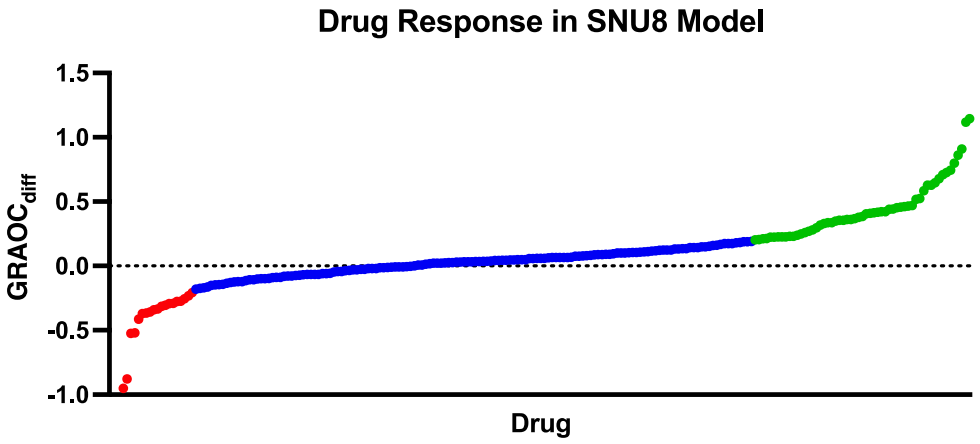

Figure 11. GRAOC Difference Results of Library Screen in SNU8 Model (OKL and OvCa-L), biological replicate two of three.

Description of figure 11, Results of the screen, $GRAOC_{diff}$ of each drug against SNU8-P and -PR are denoted as "Cross Resistant" (GRAOCdiff ≤ -0.2) in red, "No Change" (-0.2<$GRAOC_{diff}$< 0.2) in blue, and "Sensitive" ($GRAOC_{diff}$ ≥0.2) in green. Figure depicts biological replicate 2 of 3.

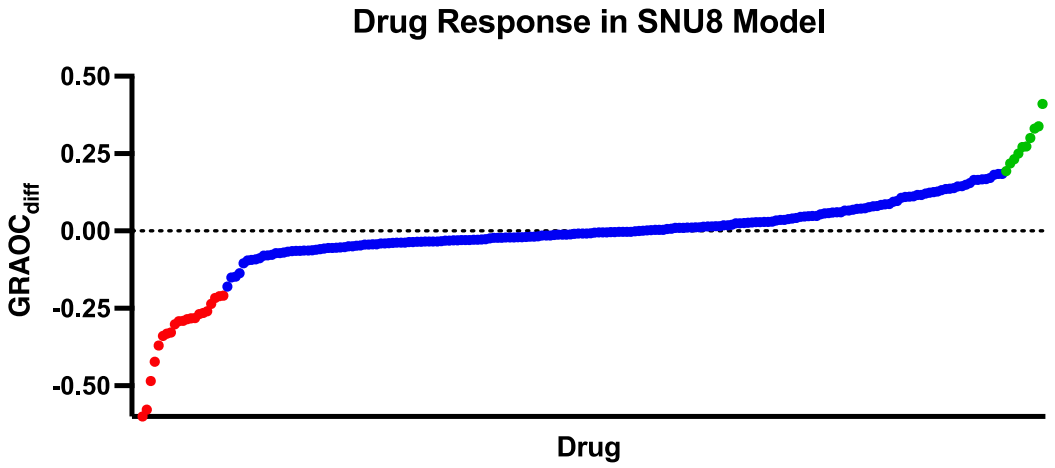

Figure 12. GRAOC Difference Results of Library Screen in SNU8 Model (OKL and OvCa-L), biological replicate three of three.

Description of figure 12, Description of figure 10, Results of the screen, $GRAOC_{diff}$ of each drug against SNU8-P and -PR are denoted as "Cross Resistant" (GRAOCdiff ≤ -0.2) in red, "No Change" (-0.2<$GRAOC_{diff}$< 0.2) in blue, and "Sensitive" ($GRAOC_{diff}$ ≥0.2) in green. Figure depicts biological replicate 3 of 3.

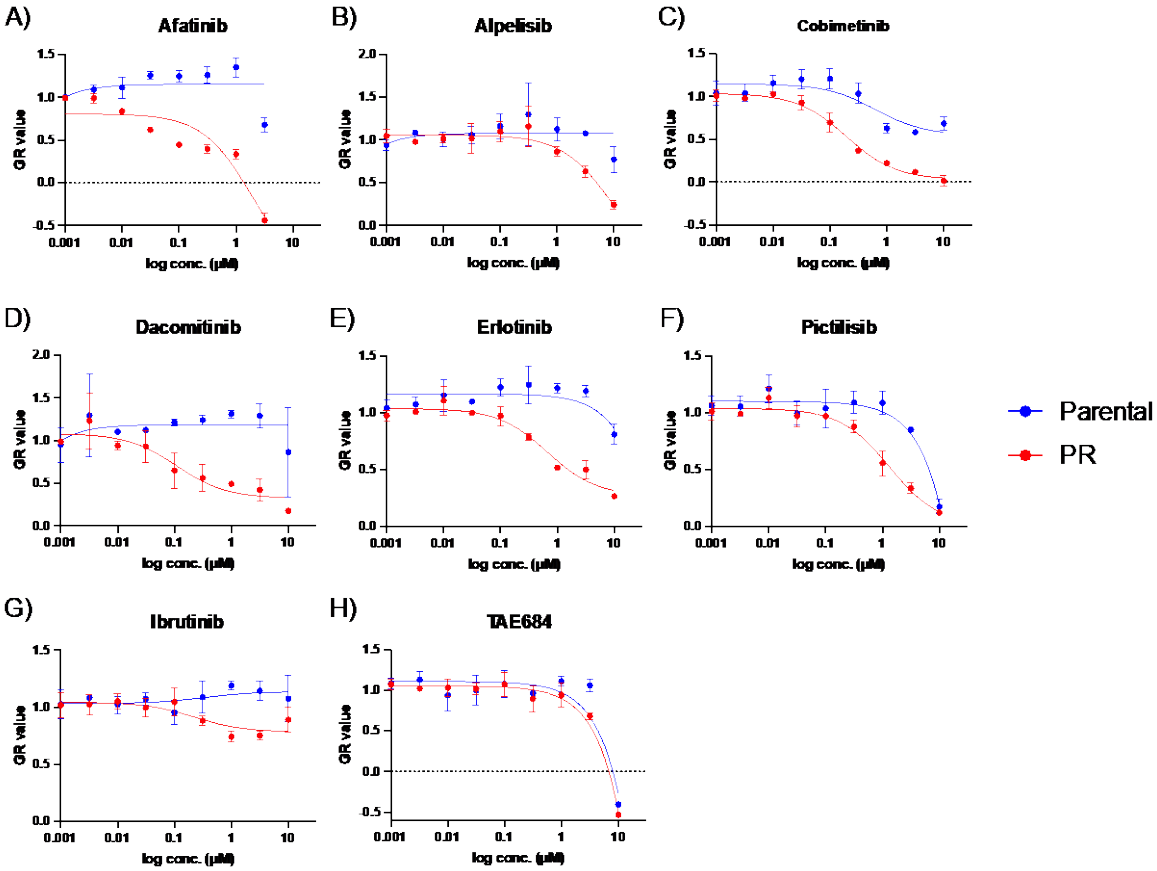

Figure 13. Dose Response of Parental and PR Cell Lines in response to top 8 drug hits.

Description of Figure 13, nonlinear regression (curve fit) of concentration of A) afatinib, B) alpelisib, C) cobimetinib, D) dacomitinib, E) erlotinib, F) pictilisib, G) ibrutinib and H) TAE684 versus GR response of SNU8-P (blue) and SNU8-PR (red). Data from additional replicate.

References

Anastassiadis, T., Deacon, S. W., Devarajan, K., Ma, H., & Peterson, J. R. (2011). Comprehensive assay of kinase catalytic activity reveals features of kinase inhibitor selectivity. *Nature Biotechnology*, *29*(11), 1039–1045. https://doi.org/10.1038/nbt.2017

Banerjee, S., & Kaye, S. B. (2013). New Strategies in the Treatment of Ovarian Cancer: Current Clinical Perspectives and Future Potential. *Clinical Cancer Research*, *19*(5), 961–968. https://doi.org/10.1158/1078-0432.CCR-12-2243

Barr, M. P., Gray, S. G., Hoffmann, A. C., Hilger, R. A., Thomale, J., O'Flaherty, J. D., Fennell, D. A., Richard, D., O'Leary, J. J., & O'Byrne, K. J. (2013). Generation and Characterisation of Cisplatin-Resistant Non-Small Cell Lung Cancer Cell Lines Displaying a Stem-Like Signature. *PLoS ONE*, *8*(1), e54193. https://doi.org/10.1371/journal.pone.0054193

Bray, M.-A., Singh, S., Han, H., Davis, C. T., Borgeson, B., Hartland, C., Kost-Alimova, M., Gustafsdottir, S. M., Gibson, C. C., & Carpenter, A. E. (2016). Cell Painting, a high-content image-based assay for morphological profiling using multiplexed fluorescent dyes. *Nature Protocols*, *11*(9), 1757–1774. https://doi.org/10.1038/nprot.2016.105

Cai, Y., Tan, X., Liu, J., Shen, Y., Wu, D., Ren, M., Huang, P., & Yu, D. (2014). Inhibition of PI3K/Akt/mTOR signaling pathway enhances the sensitivity of the SKOV3/DDP ovarian cancer cell line to cisplatin in vitro. *Chinese Journal of Cancer Research = Chung-Kuo Yen Cheng Yen Chiu*, *26*(5), 564–572. https://doi.org/10.3978/j.issn.1000-9604.2014.08.20

Cancer Facts & Figures 2022. (2022). *American Cancer Society.* https://www.cancer.org/cancer/ovarian-cancer/about/key-statistics.html#references

Chen, Y., Cao, X.-Y., Li, Y.-N., Qiu, Y.-Y., Li, Y.-N., Li, W., & Wang, H. (2018). Reversal of cisplatin resistance by microRNA-139-5p-independent RNF2 downregulation and MAPK inhibition in ovarian cancer. *American Journal of Physiology-Cell Physiology*, *315*(2), C225–C235. https://doi.org/10.1152/ajpcell.00283.2017

Christie, E. L., Fereday, S., Doig, K., Pattnaik, S., Dawson, S.-J., & Bowtell, D. D. L. (2017). Reversion of BRCA1/2 Germline Mutations Detected in Circulating Tumor DNA From Patients With High-Grade Serous Ovarian Cancer. *Journal of Clinical Oncology: Official Journal of the American Society of Clinical Oncology*, *35*(12), 1274–1280. https://doi.org/10.1200/JCO.2016.70.4627

Cooke, S. L., & Brenton, J. D. (2011). Evolution of platinum resistance in high-grade serous ovarian cancer. *The Lancet Oncology*, *12*(12), 1169–1174. https://doi.org/10.1016/S1470-2045(11)70123-1

Dasari, S., & Tchounwou, P. B. (2014). Cisplatin in cancer therapy: Molecular mechanisms of action. *European Journal of Pharmacology*, *740*, 364–378. https://doi.org/10.1016/j.ejphar.2014.07.025

Davis, M. I., Hunt, J. P., Herrgard, S., Ciceri, P., Wodicka, L. M., Pallares, G., Hocker, M., Treiber, D. K., & Zarrinkar, P. P. (2011). Comprehensive analysis of kinase inhibitor selectivity. *Nature Biotechnology*, *29*(11), 1046–1051. https://doi.org/10.1038/nbt.1990

Deng, J., Bai, X., Feng, X., Ni, J., Beretov, J., Graham, P., & Li, Y. (2019). Inhibition of PI3K/Akt/mTOR signaling pathway alleviates ovarian cancer chemoresistance through reversing epithelial-mesenchymal transition and decreasing cancer stem cell marker expression. *BMC Cancer*, *19*(1), 618. https://doi.org/10.1186/s12885-019-5824-9

Domcke, S., Sinha, R., Levine, D. A., Sander, C., & Schultz, N. (2013). Evaluating cell lines as tumour models by comparison of genomic profiles. *Nature Communications*, *4*(1), 2126. https://doi.org/10.1038/ncomms3126

Duan, M., Ulibarri, J., Liu, K. J., & Mao, P. (2020). Role of Nucleotide Excision Repair in Cisplatin Resistance. *International Journal of Molecular Sciences*, *21*(23), 9248. https://doi.org/10.3390/ijms21239248

Ediriweera, M. K., Tennekoon, K. H., & Samarakoon, S. R. (2019). Role of the PI3K/AKT/mTOR signaling pathway in ovarian cancer: Biological and therapeutic significance. *Seminars in Cancer Biology*, *59*, 147–160. https://doi.org/10.1016/j.semcancer.2019.05.012

Fabian, M. A., Biggs, W. H., Treiber, D. K., Atteridge, C. E., Azimioara, M. D., Benedetti, M. G., Carter, T. A., Ciceri, P., Edeen, P. T., Floyd, M., Ford, J. M., Galvin, M., Gerlach, J. L., Grotzfeld, R. M., Herrgard, S., Insko, D. E., Insko, M. A., Lai, A. G., Lélias, J.-M., … Lockhart, D. J. (2005). A small molecule–kinase interaction map for clinical kinase inhibitors. *Nature Biotechnology*, *23*(3), 329–336. https://doi.org/10.1038/nbt1068

Fraser, M., Bai, T., & Tsang, B. K. (2008). Akt promotes cisplatin resistance in human ovarian cancer cells through inhibition of p53 phosphorylation and nuclear

function. *International Journal of Cancer*, *122*(3), 534–546. https://doi.org/10.1002/ijc.23086

Galluzzi, L., Senovilla, L., Vitale, I., Michels, J., Martins, I., Kepp, O., Castedo, M., & Kroemer, G. (2012). Molecular mechanisms of cisplatin resistance. *Oncogene*, *31*(15), 1869–1883. https://doi.org/10.1038/onc.2011.384

Gershenson, D. M., Miller, A., Brady, W., Paul, J., Carty, K., Rodgers, W., Millan, D., Coleman, R. L., Moore, K. N., Banerjee, S., Connolly, K., Secord, A. A., O'Malley, D. M., Dorigo, O., Gaillard, S., Gabra, H., Hanjani, P., Huang, H., Wenzel, L., & Gourley, C. (2019). A randomized phase II/III study to assess the efficacy of trametinib in patients with recurrent or progressive low-grade serous ovarian or peritoneal cancer. *Annals of Oncology*, *30*, v897–v898. https://doi.org/10.1093/annonc/mdz394.058

Hafner, M., Niepel, M., Chung, M., & Sorger, P. K. (2016). Growth rate inhibition metrics correct for confounders in measuring sensitivity to cancer drugs. *Nature Methods*, *13*(6), 521–527. https://doi.org/10.1038/nmeth.3853

Hafner, M., Niepel, M., & Sorger, P. K. (2017). Alternative drug sensitivity metrics improve preclinical cancer pharmacogenomics. *Nature Biotechnology*, *35*(6), 500–502. https://doi.org/10.1038/nbt.3882

Hua, H., Zhang, H., Chen, J., Wang, J., Liu, J., & Jiang, Y. (2021). Targeting Akt in cancer for precision therapy. *Journal of Hematology & Oncology*, *14*(1), 128. https://doi.org/10.1186/s13045-021-01137-8

Iyengar, M., O'Hayer, P., Cole, A., Sebastian, T., Yang, K., Coffman, L., & Buckanovich, R. J. (2018). CDK4/6 inhibition as maintenance and combination

therapy for high grade serous ovarian cancer. *Oncotarget*, *9*(21), 15658–15672. https://doi.org/10.18632/oncotarget.24585

Kampan, N. C., Madondo, M. T., McNally, O. M., Quinn, M., & Plebanski, M. (2015). Paclitaxel and Its Evolving Role in the Management of Ovarian Cancer. *BioMed Research International*, *2015*, 413076. https://doi.org/10.1155/2015/413076

Kim, A., Ueda, Y., Naka, T., & Enomoto, T. (2012). Therapeutic strategies in epithelial ovarian cancer. *Journal of Experimental & Clinical Cancer Research*, *31*(1), 14. https://doi.org/10.1186/1756-9966-31-14

Konstantinopoulos, P. A., Ceccaldi, R., Shapiro, G. I., & D'Andrea, A. D. (2015). Homologous Recombination Deficiency: Exploiting the Fundamental Vulnerability of Ovarian Cancer. *Cancer Discovery*, *5*(11), 1137–1154. https://doi.org/10.1158/2159-8290.CD-15-0714

Kristedja, T., Morgan, R., & Cristea, M. (2010). Targeted Agents in Ovarian Cancer. *Women's Health*, *6*(5), 679–694. https://doi.org/10.2217/WHE.10.48

Lisio, M.-A., Fu, L., Goyeneche, A., Gao, Z., & Telleria, C. (2019). High-Grade Serous Ovarian Cancer: Basic Sciences, Clinical and Therapeutic Standpoints. *International Journal of Molecular Sciences*, *20*(4), 952. https://doi.org/10.3390/ijms20040952

Liu, M., Qi, Z., Liu, B., Ren, Y., Li, H., Yang, G., & Zhang, Q. (2015). RY-2f, an isoflavone analog, overcomes cisplatin resistance to inhibit ovarian tumorigenesis via targeting the PI3K/AKT/mTOR signaling pathway. *Oncotarget*, *6*(28), 25281–25294. https://doi.org/10.18632/oncotarget.4634

Masters, J. R., Thomson, J. A., Daly-Burns, B., Reid, Y. A., Dirks, W. G., Packer, P., Toji, L. H., Ohno, T., Tanabe, H., Arlett, C. F., Kelland, L. R., Harrison, M., Virmani, A., Ward, T. H., Ayres, K. L., & Debenham, P. G. (2001). Short tandem repeat profiling provides an international reference standard for human cell lines. *Proceedings of the National Academy of Sciences of the United States of America*, *98*(14), 8012–8017. https://doi.org/10.1073/pnas.121616198

McClung, E. C., & Wenham, R. M. (2016). Profile of bevacizumab in the treatment of platinum-resistant ovarian cancer: Current perspectives. *International Journal of Women's Health*, *8*, 59–75. https://doi.org/10.2147/IJWH.S78101

Michels, J., Vitale, I., Galluzzi, L., Adam, J., Olaussen, K. A., Kepp, O., Senovilla, L., Talhaoui, I., Guegan, J., Enot, D. P., Talbot, M., Robin, A., Girard, P., Oréar, C., Lissa, D., Sukkurwala, A. Q., Garcia, P., Behnam-Motlagh, P., Kohno, K., … Kroemer, G. (2013). Cisplatin Resistance Associated with PARP Hyperactivation. *Cancer Research*, *73*(7), 2271–2280. https://doi.org/10.1158/0008-5472.CAN-12-3000

Mills, C. E., Subramanian, K., Hafner, M., Niepel, M., Gerosa, L., Chung, M., Victor, C., Gaudio, B., Yapp, C., Nirmal, A. J., Clark, N., & Sorger, P. K. (2022). Multiplexed and reproducible high content screening of live and fixed cells using Dye Drop. *Nature Communications*, *13*(1), 6918. https://doi.org/10.1038/s41467-022-34536-7

Moghbeli, M. (2021). MicroRNAs as the critical regulators of Cisplatin resistance in ovarian cancer cells. *Journal of Ovarian Research*, *14*(1), 127. https://doi.org/10.1186/s13048-021-00882-1

Momeny, M., Zarrinrad, G., Moghaddaskho, F., Poursheikhani, A., Sankanian, G., Zaghal, A., Mirshahvaladi, S., Esmaeili, F., Eyvani, H., Barghi, F., Sabourinejad, Z., Alishahi, Z., Yousefi, H., Ghasemi, R., Dardaei, L., Bashash, D., Chahardouli, B., Dehpour, A. R., Tavakkoly-Bazzaz, J., … Ghaffari, S. H. (2017). Dacomitinib, a pan-inhibitor of ErbB receptors, suppresses growth and invasive capacity of chemoresistant ovarian carcinoma cells. *Scientific Reports*, *7*(1), 4204. https://doi.org/10.1038/s41598-017-04147-0

Moret, N., Clark, N. A., Hafner, M., Wang, Y., Lounkine, E., Medvedovic, M., Wang, J., Gray, N., Jenkins, J., & Sorger, P. K. (2019). Cheminformatics Tools for Analyzing and Designing Optimized Small-Molecule Collections and Libraries. *Cell Chemical Biology*, *26*(5), 765-777.e3. https://doi.org/10.1016/j.chembiol.2019.02.018

Moret, N., Liu, C., Gyori, B. M., Bachman, J. A., Steppi, A., Hug, C., Taujale, R., Huang, L.-C., Berginski, M. E., Gomez, S. M., Kannan, N., & Sorger, P. K. (2020). A resource for exploring the understudied human kinome for research and therapeutic opportunities [Preprint]. *Systems Biology*. https://doi.org/10.1101/2020.04.02.022277

Mullard, A. (2024). FDA approves first-in-class AKT inhibitor. *Nature Reviews Drug Discovery*, *23*(1), 9–9. https://doi.org/10.1038/d41573-023-00202-w

Murai, J., Huang, S.-Y. N., Renaud, A., Zhang, Y., Ji, J., Takeda, S., Morris, J., Teicher, B., Doroshow, J. H., & Pommier, Y. (2014). Stereospecific PARP trapping by BMN 673 and comparison with olaparib and rucaparib. *Molecular Cancer Therapeutics*, *13*(2), 433–443. https://doi.org/10.1158/1535-7163.MCT-13-0803

Niepel, M., Hafner, M., Mills, C. E., Subramanian, K., Williams, E. H., Chung, M., Gaudio, B., Barrette, A. M., Stern, A. D., Hu, B., Korkola, J. E., LINCS Consortium, Gray, J. W., Birtwistle, M. R., Heiser, L. M., & Sorger, P. K. (2019). A Multi-center Study on the Reproducibility of Drug-Response Assays in Mammalian Cell Lines. *Cell Systems*, *9*(1), 35-48.e5. https://doi.org/10.1016/j.cels.2019.06.005

Noah, J. W., Severson, W., Noah, D. L., Rasmussen, L., White, E. L., & Jonsson, C. B. (2007). A cell-based luminescence assay is effective for high-throughput screening of potential influenza antivirals. *Antiviral Research*, *73*(1), 50–59. https://doi.org/10.1016/j.antiviral.2006.07.006

Odogwu, L., Mathieu, L., Blumenthal, G., Larkins, E., Goldberg, K. B., Griffin, N., Bijwaard, K., Lee, E. Y., Philip, R., Jiang, X., Rodriguez, L., McKee, A. E., Keegan, P., & Pazdur, R. (2018). FDA Approval Summary: Dabrafenib and Trametinib for the Treatment of Metastatic Non-Small Cell Lung Cancers Harboring *BRAF V600E* Mutations. *The Oncologist*, *23*(6), 740–745. https://doi.org/10.1634/theoncologist.2017-0642

Peng, D.-J., Wang, J., Zhou, J.-Y., & Wu, G. S. (2010). Role of the Akt/mTOR survival pathway in cisplatin resistance in ovarian cancer cells. *Biochemical and Biophysical Research Communications*, *394*(3), 600–605. https://doi.org/10.1016/j.bbrc.2010.03.029

Poursheikhani, A., Yousefi, H., Tavakoli-Bazzaz, J., & Seyed H, G. (2020). EGFR Blockade Reverses Cisplatin Resistance in Human Epithelial Ovarian Cancer

Cells. *Iranian Biomedical Journal*, *24*(6), 370–378. https://doi.org/10.29252/ibj.24.6.365

Ren, L., Xiao, L., Hu, J., Li, Z., & Wang, Z. (2007). MDR1 and MDR3 genes and drug resistance to cisplatin of ovarian cancer cells. *Journal of Huazhong University of Science and Technology [Medical Sciences]*, *27*(6), 721–724. https://doi.org/10.1007/s11596-007-0627-7

Rodrigues Moita, A. J., Bandolik, J. J., Hansen, F. K., Kurz, T., Hamacher, A., & Kassack, M. U. (2020). Priming with HDAC Inhibitors Sensitizes Ovarian Cancer Cells to Treatment with Cisplatin and HSP90 Inhibitors. *International Journal of Molecular Sciences*, *21*(21), 8300. https://doi.org/10.3390/ijms21218300

Sanders, B. E., Yamamoto, T. M., McMellen, A., Woodruff, E. R., Berning, A., Post, M. D., & Bitler, B. G. (2022). Targeting DUSP Activity as a Treatment for High-Grade Serous Ovarian Carcinoma. *Molecular Cancer Therapeutics*, *21*(8), 1285–1295. https://doi.org/10.1158/1535-7163.MCT-21-0682

Shaffer, S. M., Dunagin, M. C., Torborg, S. R., Torre, E. A., Emert, B., Krepler, C., Beqiri, M., Sproesser, K., Brafford, P. A., Xiao, M., Eggan, E., Anastopoulos, I. N., Vargas-Garcia, C. A., Singh, A., Nathanson, K. L., Herlyn, M., & Raj, A. (2017). Rare cell variability and drug-induced reprogramming as a mode of cancer drug resistance. *Nature*, *546*(7658), 431–435. https://doi.org/10.1038/nature22794

Sherman-Baust, C. A., Becker, K. G., Wood Iii, W. H., Zhang, Y., & Morin, P. J. (2011). Gene expression and pathway analysis of ovarian cancer cells selected for

resistance to cisplatin, paclitaxel, or doxorubicin. *Journal of Ovarian Research*, *4*(1), 21. https://doi.org/10.1186/1757-2215-4-21

Sima, N., Sun, W., Gorshkov, K., Shen, M., Huang, W., Zhu, W., Xie, X., Zheng, W., & Cheng, X. (2018). Small Molecules Identified from a Quantitative Drug Combinational Screen Resensitize Cisplatin's Response in Drug-Resistant Ovarian Cancer Cells. *Translational Oncology*, *11*(4), 1053–1064. https://doi.org/10.1016/j.tranon.2018.06.002

Singh, S., Bradford, D., Li, X., Mishra-Kalyani, P. S., Shen, Y.-L., Wang, L., Zhao, H., Xiong, Y., Liu, J., Charlab, R., Kraft, J., Khasar, S., Miller, C. P., Rivera, D. R., Kluetz, P. G., Pazdur, R., Beaver, J. A., Singh, H., & Donoghue, M. (2024). FDA Approval Summary: Alpelisib for PIK3CA-Related Overgrowth Spectrum. *Clinical Cancer Research*, *30*(1), 23–28. https://doi.org/10.1158/1078-0432.CCR-23-1270

Siwak, D. R., Carey, M., Hennessy, B. T., Nguyen, C. T., McGahren Murray, M. J., Nolden, L., & Mills, G. B. (2010). Targeting the Epidermal Growth Factor Receptor in Epithelial Ovarian Cancer: Current Knowledge and Future Challenges. *Journal of Oncology*, *2010*, 1–20. https://doi.org/10.1155/2010/568938

Song, M., Cui, M., & Liu, K. (2022). Therapeutic strategies to overcome cisplatin resistance in ovarian cancer. *European Journal of Medicinal Chemistry*, *232*, 114205. https://doi.org/10.1016/j.ejmech.2022.114205

Tian, C., Yang, C., & Spencer, S. L. (2020). EllipTrack: A Global-Local Cell-Tracking Pipeline for 2D Fluorescence Time-Lapse Microscopy. *Cell Reports*, *32*(5), 107984. https://doi.org/10.1016/j.celrep.2020.107984

Turke, A. B., Song, Y., Costa, C., Cook, R., Arteaga, C. L., Asara, J. M., & Engelman, J. A. (2012). MEK Inhibition Leads to PI3K/AKT Activation by Relieving a Negative Feedback on ERBB Receptors. *Cancer Research*, *72*(13), 3228–3237. https://doi.org/10.1158/0008-5472.CAN-11-3747

Vanderstichele, A., Van Nieuwenhuysen, E., Han, S., Concin, N., Van Gorp, T., Berteloot, P., Neven, P., Busschaert, P., Lambrechts, D., & Vergote, I. (2019). Randomized phase II CLIO study on olaparib monotherapy versus chemotherapy in platinum-resistant ovarian cancer. *Journal of Clinical Oncology*, *37*(15_suppl), 5507–5507. https://doi.org/10.1200/JCO.2019.37.15_suppl.5507

Wang, H., Yu, Y., Chen, C., Wang, Q., Huang, T., Hong, F., & Zhu, L. (2015). Involvement of enhancer of zeste homolog 2 in cisplatin-resistance in ovarian cancer cells by interacting with several genes. *Molecular Medicine Reports*, *12*(2), 2503–2510. https://doi.org/10.3892/mmr.2015.3745

Wang, J., Kho, D. H., Zhou, J.-Y., Davis, R. J., & Wu, G. S. (2017). MKP-1 suppresses PARP-1 degradation to mediate cisplatin resistance. *Oncogene*, *36*(43), 5939–5947. https://doi.org/10.1038/onc.2017.197

Wang, S., Liu, S., Zhao, B., Yang, F., Wang, Y., Liang, Q.-Y., Sun, Y., Liu, Y., Song, Z., Cai, Y., & Li, G. (2015). Afatinib reverses multidrug resistance in ovarian cancer via dually inhibiting ATP binding cassette subfamily B member 1. *Oncotarget*, *6*(28), 26142–26160. https://doi.org/10.18632/oncotarget.4536

Wee, P., & Wang, Z. (2017). Epidermal Growth Factor Receptor Cell Proliferation Signaling Pathways. *Cancers*, *9*(5), E52. https://doi.org/10.3390/cancers9050052

Wilken, J. A., Badri, T., Cross, S., Raji, R., Santin, A. D., Schwartz, P., Branscum, A. J., Baron, A. T., Sakhitab, A. I., & Maihle, N. J. (2012). EGFR/HER-targeted therapeutics in ovarian cancer. *Future Medicinal Chemistry*, *4*(4), 447–469. https://doi.org/10.4155/fmc.12.11

Xu, L., Xu, Y., Zheng, J., Zhao, Y., Wang, H., & Qi, Y. (2021). Dacomitinib improves chemosensitivity of cisplatin-resistant human ovarian cancer cells. *Oncology Letters*, *22*(1), 569. https://doi.org/10.3892/ol.2021.12830

Yang, L., Zhao, H., Yin, X., Liang, H., Zheng, Z., Shen, Q., & Hu, W. (2020). Exploring cisplatin resistance in ovarian cancer through integrated bioinformatics approach and overcoming chemoresistance with sanguinarine. *American Journal of Translational Research*, *12*(3), 923–939.

Zhang, H., Christensen, C. L., Dries, R., Oser, M. G., Deng, J., Diskin, B., Li, F., Pan, Y., Zhang, X., Yin, Y., Papadopoulos, E., Pyon, V., Thakurdin, C., Kwiatkowski, N., Jani, K., Rabin, A. R., Castro, D. M., Chen, T., Silver, H., … Wong, K.-K. (2020). CDK7 Inhibition Potentiates Genome Instability Triggering Anti-tumor Immunity in Small Cell Lung Cancer. *Cancer Cell*, *37*(1), 37-54.e9. https://doi.org/10.1016/j.ccell.2019.11.003

Zhang, J., Kan, Y., Tian, Y., Wang, Z., & Zhang, J. (2013). Effects of poly (ADP-ribosyl) polymerase (PARP) inhibitor on cisplatin resistance & proliferation of the ovarian cancer C13* cells. *The Indian Journal of Medical Research*, *137*(3), 527–532.